

# Bayesian Adaptive Selection of Variables for Function-on-Scalar Regression Models

Pedro Henrique T. O. Sousa<sup>1\*</sup>, Camila P. E. de Souza<sup>2</sup>, Ronaldo Dias<sup>1</sup>

<sup>1</sup>Department of Statistics, University of Campinas, SP, Brazil

<sup>2</sup>Department of Statistical and Actuarial Sciences, University of Western Ontario, ON, Canada

\*Correspondence: phtos.est@gmail.com

## Abstract

Considering the field of functional data analysis, we developed a new Bayesian method for variable selection in function-on-scalar regression (FOSR). Our approach uses latent variables and a hierarchical Bayesian structure, allowing an adaptive selection of covariates for a FOSR model. Simulation studies show the proposed method's main properties, such as its accuracy in estimating the coefficients and high capacity to select variables correctly. Furthermore, we conducted comparative studies with the main competing methods, such as the BGLSS method as well as the group LASSO, the group MCP and the group SCAD. We also used a COVID-19 dataset and some socio-economic data from Brazil for real data application. In short, the proposed Bayesian variable selection model is extremely competitive, showing significant predictive and selective quality.

**Keywords:** Bayesian inference, functional data, functional data analysis, variable selection, latent variable, function-on-scalar regression.

## 1 Introduction

Linear regression models are already well consolidated, and well understood in the statistical literature (Weisberg, 2013; Rencher and Schaalje, 2008; Kutner et al., 2004), with most models developed considering cross-sectional rather than functional data. When the data are functions, the standard linear regression models, generally, cannot be used directly because they require building of a design matrix that contains not only the covariates information but also other important elements, such as the basis functions coming from the expansions of the functional data. This strategy can be observed in some works such as in Wang et al. (2007), Chen et al. (2016) and Barber et al. (2017). Functional regression (Ramsay and Silverman, 2005; Chapters 12 to 17) then emerged to circumvent this problem, being one of the areas of functional data analysis that has received a lot of attention, both in applied studies and in methodological developments (Qi and Luo, 2018; Meyer et al., 2015; Reiss et al., 2017; Chen et al., 2016; Horváth and Kokoszka, 2012; Ramsay and Silverman, 2005; among others).

It is worth to mention three types of functional regression modeling as mentioned in Ramsay and Silverman (2005): *i*) the functional predictor regression (*scalar-on-function*), in which covariates and coefficients are functional but the response is not; *ii*) the regression with functional response (*function-on-scalar*), where the covariates are vectors and the coefficients are functional; *iii*) and the regression that models the association through

functional coefficients, between functional covariates and a functional response (*function-on-function*).

Bearing in mind the context of functional regression and the growing demand for selection models in this area, herein we focus on a regression problem of the *function-on-scalar* type and propose a Bayesian selection model of covariates. In what follows, we describe in more details the proposed function-on-scalar regression (FOSR) model (*ii*). For a description of the other types of modeling (*i* and *iii* described above), see Ramsay and Silverman (2005).

In function-on-scalar regression (FOSR), we consider a set of scalar predictor variables  $x_{li}$ , where  $i$  is the index linked to the  $i$ th curve and  $l$  is the one associated with the  $l$ th covariate. Then, considering a linear structure, we have the following model:

$$y_i(t) = \beta_0(t) + \sum_{l=1}^p x_{li}\beta_l(t) + \epsilon_i(t). \quad (1)$$

So, it is also necessary to impose some kind of regularization to avoid overfitting. Notice that the intercept and variable coefficients are functional. The component  $\epsilon_i(t)$  represents the error curve, or residual curve. It is often assumed that the error curves are independent, and come from the same Gaussian process with a mean of zero and a given covariance structure.

In many cases, in addition to the goal on prediction, the aim is to establish a good estimation of the functional coefficients in (1), assessing whether  $\beta_l(t) = 0$  for all  $t$  for some  $l$ , or even checking whether a given functional coefficient is null only at specific points, meaning if  $\beta_l(t) = 0$  only for some values of  $t$ .

The literature on variable selection in functional regression analysis is still not dominant. However, there is strong evidence that this area has grown rapidly in recent years, especially in the last decade. Some examples of variable selection in functional regression can be found in Matsui and Konishi (2011), which studied the group SCAD regularization for the selection of functional regressors, Mingotti et al. (2013) and Hong and Lian (2011), which generalized LASSO to the case of scalar covariates and functional response, among others (Collazos et al., 2016; Fan and Li, 2004; Aneiros et al., 2011; Gertheiss et al., 2013; Ma et al., 2013).

There is, specifically, a growing interest in research problems on function *function-on-scalar regression* (FOSR). Some works from the last decade explore the potential of FOSR under a Bayesian perspective, as can be seen in Montagna et al. (2012) and in Kowal (2018), as well as Kowal and Bourgeois (2020), which additionally handles variable selection. However, the frequentist approach is predominant when it comes to variable selection in FOSR. Several studies with a focus on variable selection in FOSR were developed and applied to genetic datasets (Wang et al., 2007; Fan and Reimherr, 2017; Barber et al., 2017; Parodi and Reimherr, 2018), although there are other areas of applications, such as for Alzheimer's data (CAI et al., 2022), among others (Chen et al., 2016; Kowal and Bourgeois, 2020).

In this work, we propose a new Bayesian approach to select covariates in a FOSR model by associating a Bernoulli latent variable to each functional coefficient, making it possible to assign zero to certain model functional coefficients with a positive probability. From a hierarchical structure, we obtain the full conditional distributions used in a Gibbs sampler to sample from the posterior distribution. This proposed methodology is inspired by the work of (de Oliveira Sousa et al., 2023), in which we developed a Bayesian approach to select basis functions for functional data representation.

This paper is organized as follows. Section 2 presents the proposed Bayesian model for variable selection in FOSR, while Section 3 shows the design and results of several numerical experiments involving the proposed methodology. Also, in Section 3, we present a comparative study between the proposed model and the methods *group LASSO*, *group SCAD*, *group MCP* and *BGLSS*. In Section 4, we conduct a study to evaluate the performance of the proposed model in a functional regression problem involving some socioeconomic data and COVID-19 data from the Federal District and Brazilian states. Finally, Section 5 provides some general conclusions about this work.

## 2 Proposed Bayesian model for variable selection in functional regression

For the introduction of the proposed Bayesian model, let us consider  $p$  covariates,  $m$  curves with  $n_i$  observations at the points  $t_{ij} \in A \subseteq \mathbb{R}$ , in which  $i \in \{1, 2, \dots, m\}$  and  $j \in \{1, 2, \dots, n_i\}$ . So, we assume that:

$$y_{ij} = \beta_0(t_{ij}) + \sum_{l=1}^p x_{li} Z_l \beta_l(t_{ij}) + \epsilon_{ij}, \quad (2)$$

where  $Z_l$  is a Bernoulli latent variable that will select or not the  $l$ th covariate. While  $y_{ij}$  represents the value of the  $i$ th curve at point  $t_{ij}$  (meaning  $y_{ij} = y_i(t_{ij})$ ), the partial functional coefficients associated with the covariates are represented by  $\beta_l(\cdot)$ 's, just as  $\beta_0(\cdot)$  represents the intercept. Finally,  $\epsilon_{ij} = \epsilon_i(t_{ij})$  is the random component that represents the error measurements with a normal distribution with zero mean and variance equal to  $\sigma^2$ .

For a given fixed curve  $i$ , the vector with the final functional coefficients of this functional linear regression is given by  $\boldsymbol{\nu}(\cdot) = (\nu_1(\cdot), \nu_2(\cdot), \dots, \nu_p(\cdot))' = (Z_1 \beta_1(\cdot), Z_2 \beta_2(\cdot), \dots, Z_p \beta_p(\cdot))'$ . For the sake of brevity and to avoid confusion in the notation, the components  $\nu_l(\cdot)$ 's will be called functional coefficients, while the  $\beta_l(\cdot)$ 's will be called partial functional coefficients.

We carry out a basis function expansion for all  $\beta_l(\cdot)$ 's and  $\beta_0(\cdot)$  in (2) with the same set of known basis functions,  $B_1(\cdot), \dots, B_K(\cdot)$ , as follows:

$$\begin{aligned} y_{ij} &= \sum_{k=1}^K b_{k0} B_k(t_{ij}) + \sum_{l=1}^p x_{li} Z_l \left[ \sum_{k=1}^K b_{kl} B_k(t_{ij}) \right] + \epsilon_{ij} \\ &= \sum_{k=1}^K b_{k0} B_k(t_{ij}) + \sum_{l=1}^p \sum_{k=1}^K x_{li} Z_l b_{kl} B_k(t_{ij}) + \epsilon_{ij}, \end{aligned}$$

where the  $b_{kl}$ 's represent the coefficients of the basis expansion for the  $l$ th partial functional coefficient, and the  $b_{k0}$ 's are the coefficients of the basis expansion applied on the functional intercept.

Hence, developing the Bayesian model for adaptive variable selection through a hierarchical structure is possible. First, however, some definitions should be established for ease of understanding. Let  $\boldsymbol{\theta} = (\theta_1, \theta_2, \dots, \theta_p)'$  and  $\mathbf{Z} = (Z_1, Z_2, \dots, Z_p)'$ . While  $\boldsymbol{\theta}$  and  $\mathbf{Z}$  are vectors of dimension  $(p \times 1)$ , there are two other vectors of higher dimension  $(Kp \times 1)$  that are:  $\boldsymbol{\tau}^2 = (\boldsymbol{\tau}_1^2, \boldsymbol{\tau}_2^2, \dots, \boldsymbol{\tau}_p^2)'$ , where  $\boldsymbol{\tau}_l^2 = (\tau_{1l}^2, \tau_{2l}^2, \dots, \tau_{Kl}^2)'$  and  $\mathbf{b} = (\mathbf{b}_{.1}, \mathbf{b}_{.2}, \dots, \mathbf{b}_{.p})'$ , with  $\mathbf{b}_{.l} = (b_{1l}, b_{2l}, \dots, b_{Kl})'$ . Note that there is also a vector that contains all  $b_{k0}$ 's, say,  $\mathbf{b}_0 = (b_{10}, b_{20}, \dots, b_{K0})'$ . It is worth mentioning that the intercept will be estimated separately; therefore, a prior will not be assigned to the  $b_{k0}$ 's.

Finally, consider  $\mathbf{y} = (\mathbf{y}_1.', \mathbf{y}_2.', \dots, \mathbf{y}_m.')'$ , where  $\mathbf{y}_i. = (y_{i1}, y_{i2}, \dots, y_{in_i})'$ . Then, we have:

$$\begin{aligned} y_{ij} | \mathbf{Z}, \mathbf{b}, \sigma^2 &\sim \text{N} \left( \sum_{k=1}^K b_{k0} B_k(t_{ij}) + \sum_{l=1}^p \sum_{k=1}^K x_{li} Z_l b_{kl} B_k(t_{ij}), \sigma^2 \right); \\ b_{kl} | \sigma^2, \boldsymbol{\tau}^2 &\sim \text{N}(0, \sigma^2 \tau_{kl}^2); \\ Z_l | \boldsymbol{\theta} &\sim \text{Ber}(\theta_l); \\ \theta_l | \boldsymbol{\mu} &\sim \text{Beta}(\mu_l, (1 - \mu_l)); \\ \mu_l &\sim \text{U}(0, \psi), \quad \text{in which } \psi < 1; \\ \tau_{kl}^2 &\sim \text{Exp} \left( \frac{\lambda^2}{2} \right) \quad \text{and} \quad \sigma^2 \sim \text{IG}(\delta_1, \delta_2). \end{aligned} \quad (3)$$

One can also simplify the hierarchical model in (3) by considering  $\mu_l$  as a hyperparameter, obtaining:

$$\begin{aligned} y_{ij} | \mathbf{Z}, \mathbf{b}, \sigma^2 &\sim \text{N} \left( \sum_{k=1}^K b_{k0} B_k(t_{ij}) + \sum_{l=1}^p \sum_{k=1}^K x_{li} Z_l b_{kl} B_k(t_{ij}), \sigma^2 \right); \\ b_{kl} | \sigma^2, \boldsymbol{\tau}^2 &\sim \text{N}(0, \sigma^2 \tau_{kl}^2); \\ Z_l | \boldsymbol{\theta} &\sim \text{Ber}(\theta_l); \\ \theta_l | \boldsymbol{\mu} &\sim \text{Beta}(\mu_l, (1 - \mu_l)); \\ \tau_{kl}^2 &\sim \text{Exp} \left( \frac{\lambda^2}{2} \right) \quad \text{and} \quad \sigma^2 \sim \text{IG}(\delta_1, \delta_2). \end{aligned} \quad (4)$$

A sample from the posterior distribution of  $\mathbf{Z}$ ,  $\mathbf{b}$  and  $\sigma^2$  is obtained via the Gibbs sampler described in Section 2.1.

In the model with  $\mu_l$  as a parameter, it is recommended to define  $\psi$  as a value not too close to 1 because very high values of  $\psi$  can lead to numerical issues in the implementation of the Gibbs sampler. When  $\mu_l$  is a hyperparameter, it is known that the closer  $\mu_l$  is to 0.5, the less informative will be the prior of  $\theta_l$  since in addition to having an average located precisely in the middle of the interval between 0 and 1, the respective density will be symmetric and with maximum variance. Although the  $\theta_l$  prior only explicitly presents one hyperparameter, one can rewrite  $\mu_l$  so that, for all  $l$ ,  $\mu_l = \frac{C}{p}$ , where  $C$  is a tuning parameter and can be interpreted as a prior guess about how many variables, on average, one wants to select. With this perspective, the  $\theta_l$  prior, now, has two hyperparameters,  $C$  and  $p$ . To visualize this, one can think of a prior mean of the binomial generated by the sum of the  $Z_l$ 's, that is:

$$\text{E} \left( \sum_{l=1}^p Z_l \right) = \sum_{l=1}^p \text{E}(\text{E}(Z_l | \theta_l)) = \sum_{l=1}^p \text{E}(\theta_l) = \sum_{l=1}^p \mu_l = \sum_{l=1}^p \frac{C}{p} = p \frac{C}{p} = C.$$

## 2.1 Gibbs sampler

Appendix A details how to obtain the full conditional distributions for the model given in (3) used in our Gibbs sampler. The algorithm is analogous to the model in (4). The panel 2.1 presents the standard procedure for implementing the Gibbs sampler in a clear and summarized way.

1. Define the hyperparameters;
2. Assign initial chain values to parameters;
3. For  $c = 2, \dots, N_{\text{int}}$ :
  - 3.1 Sample  $\sigma^{2(c)} \sim f(\sigma^2 | \mathbf{b}^{(c-1)}, \boldsymbol{\tau}^{2(c-1)}, \mathbf{Z}^{(c-1)}, \mathbf{y})$ , an Inverse-Gamma as in (12);
  - 3.2 For  $k = 1, \dots, K$ :
    - 3.2.1 For  $l = 1, \dots, p$ :
      - 3.2.1.1 Sample  $\eta_{kl}^{2(c)} \sim f(\eta_{kl}^2 | b_{kl}^{(c-1)}, \sigma^{2(c)})$ , an Inverse-Normal as in (14);
      - 3.2.1.2 Set  $\tau_{kl}^2 = \frac{1}{\eta_{kl}^2}$ ;
  - 3.3 For  $l = 1, \dots, p$ :
    - 3.3.1 Sample  $\mu_l^{(c)} \sim f(\mu_l | \theta_l^{(c-1)})$ , a continuous Bernoulli as in (15);
    - 3.3.2 Sample  $Z_l^{(c)}$  with  $P(Z_l = 1 | \mathbf{b}^{(c-1)}, \theta_l^{(c-1)}, \sigma^{2(c)}, \mathbf{Z}_{-[l]}^{(*)}, \mathbf{y})$  as in (11);
    - 3.3.3 Sample  $\theta_l^{(c)} \sim f(\theta_l | \mu_l^{(c)}, Z_l^{(c)})$ , a beta as in (10);
  - 3.4 Sample  $\mathbf{b}^{(c)} \sim f(\mathbf{b} | \sigma^{2(c)}, \boldsymbol{\tau}^{2(c)}, \mathbf{Z}^{(c)}, \mathbf{y})$ , a multivariate normal as in (9).

The term  $\mathbf{Z}_{-[l]}^{(*)}$  in the panel 2.1 represents a mixed vector with components from the previous iteration that have not yet been updated and with components that have already been updated in the current iteration. As  $l$  evolves in 3.3, the vector  $\mathbf{Z}_{-[l]}^{(*)}$  is updated. Also, it is worth mentioning that the complete conditional distributions are presented in the panel in summary form, since the independent components are omitted from the notation.

At the end of this process with the convergence of the chain, there is a sample of the joint posterior distribution of  $\mathbf{Z}$ ,  $\mathbf{b}$ , and  $\sigma^2$ .

### 3 Numerical experiments

Numerical experiments were carried out with synthetic data in order to assess the main properties of the proposed model. In Section 3.1, we describe details about the synthetic data generation and the Gibbs sampler implementation. Section 3.2 presents the performance metrics used for model evaluation. Then, in Section 3.3, we present the results of our numerical experiments.

#### 3.1 Synthetic data generation and Gibbs implementation

The synthetic data consists of  $m = 10$  (or  $m = 15$ ) curves generated as follows:

1. Six covariates are generated ( $X_{li}$ 's, in which  $i \in \{1, 2, \dots, m\}$  and  $l \in \{1, 2, \dots, p = 6\}$ ) represented by six vectors of  $m$  random variables such that

$$\begin{aligned}
 X_{1i} &\sim N(200, 100^2), \\
 X_{2i} &\sim N(100, 100^2), \\
 X_{3i} &\sim N(20, 50^2), \\
 X_{4i} &\sim N(50, 50^2), \\
 X_{5i} &\sim N(2, 5^2) \quad \text{and} \\
 X_{6i} &\sim N(25, 50^2);
 \end{aligned}$$

2. Define the functional coefficients

$$\begin{aligned}
 \beta_0(t) &= \exp(t^2), \\
 \beta_3(t) &= \cos(2t) \quad \text{and} \\
 \beta_5(t) &= t^3,
 \end{aligned}$$

in which  $t \in [0, 2]$ ;

3. All other partial functional coefficients do not need to be defined since it is considered that only two covariates  $X_{3i}$  and  $X_{5i}$ , should be used for data generation;
4. For each curve, a vector is defined for the error term, in which each component is represented by  $\epsilon_{ij}$  and is generated from a normal distribution with mean equal to zero and variance equal to  $\sigma^2$  (two sets of data were generated, one with  $\sigma = 0.2$  and another with  $\sigma = 20$ );
5. Fixing  $n_i = n = 25$  for the number of evaluation points in each functional and defining a common set of points  $t_{ij}$  for every functional  $i$ , which is defined by the function `seq(0, 2, length=n)` of the *software* R, the discrete representation of the  $m$  functional responses is generated such that

$$y_{ij} = y_i(t_{ij}) = \beta_0(t_{ij}) + \beta_3(t_{ij})X_{3i} + \beta_5(t_{ij})X_{5i} + \epsilon_{ij}. \quad (5)$$

The equality presented in 5 is a summary representation, since its full version is given by

$$y_{ij} = y_i(t_{ij}) = \beta_0(t_{ij}) + Z_{1i}\beta_1(t_{ij})X_{1i} + Z_{2i}\beta_2(t_{ij})X_{2i} + Z_{3i}\beta_3(t_{ij})X_{3i} + Z_{4i}\beta_4(t_{ij})X_{4i} + Z_{5i}\beta_5(t_{ij})X_{5i} + Z_{6i}\beta_6(t_{ij})X_{6i} + \epsilon_{ij}, \quad (6)$$

in which  $Z_{3i}$  and  $Z_{5i}$  are equal to one, while  $Z_{1i}$ ,  $Z_{2i}$ ,  $Z_{4i}$  and  $Z_{6i}$  are equal to zero.

The covariates chosen to compose the discrete representation (5) were purposely positioned in the design matrix  $\mathbf{X}$  so that both were not neighbors. Thus, we can verify that the model truly has the ability to select covariates and not just blocks of covariates.

Therefore, any method that performs a good fit to this dataset should be able to identify that only  $X_{3i}$  and  $X_{5i}$  are useful covariates, in addition to being able to calculate estimates for the functional coefficients which are close to the original functional parameters. When building the synthetic data, we establish that  $\beta_3(t)$  and  $\beta_5(t)$  are the so-called “functional coefficients” instead of “partial functional coefficients” since it is implied that the latent variable is equal to one in the generation of synthetic data in both cases.

Since the goal of the model is to select covariates in a functional context, we decided to direct attention to the functional coefficients associated with the covariates. In view of this, the estimation of the functional intercept took place a step prior to the model fit. Thus, the covariates were standardized by their mean and standard deviation, and the functional intercept was estimated through the functional mean of the functional responses (see Supplementary Section 1 for more details). Therefore, the result of subtracting the functional intercept estimate from the initial response variable is used as the response variable to fit the proposed model.

Bayesian inference was implemented through the Gibbs sampler described in Section 2.1 using two chains to enable the convergence diagnosis, which start at different points, and with the calculation of 10 000 iterations. Considering a *burn-in* period of 50% of the size of each chain and spacing of 50 points between each sampled value, each chain contains 100 sampled points. Thus, at the end of the process, a posterior sample of size 200 will be obtained for each parameter and latent variable.

The convergence diagnosis used in our analyses takes into account the convergence test of the chains proposed by Gelman and Rubin (1992). In our numerical experiments carried out herein, the chains were initialized as follows:

- $\mathbf{b} = -\mathbf{1}$ ,  $\boldsymbol{\theta} = \frac{1}{5}$ ,  $\sigma^2 = 1$  and  $\boldsymbol{\tau}^2 = \mathbf{1}$  for the first chain and

- $\mathbf{b} = \mathbf{1}$ ,  $\boldsymbol{\theta} = \frac{4}{5}$ ,  $\sigma^2 = 5$  and  $\boldsymbol{\tau}^2 = \mathbf{5}$  for the second chain.

The latent random variables  $Z_l$ 's were initialized in the first chain via random draw, and the complementary vector of the drawn variables for the first chain was used for the second chain.

With regard to the hyperparameters, it was defined:  $\delta_1 = \delta_2 = 0$ . Thus, when using a degenerated prior to  $\sigma^2$  with  $\delta_1 = 0$  and  $\delta_2 = 0$ , there is an equivalence with the use of a non-informative improper prior  $\frac{1}{\sigma^2}$ . Then for the hyperparameter of the priors of the  $\tau_{kl}$ 's,  $\lambda = \sqrt{2}$  was defined such that the prior mean is equal to 1. This value of  $\lambda$  is also the smallest possible value (in this data set), since uniqueness problems in the stationary distribution begin to appear for smaller values of this parameter as a result of the combination of two factors: low regularization and multicollinearity between the covariates. Therefore, there was a configuration with the lowest possible regularization.

In situations where  $\boldsymbol{\mu}$  is considered as a parameter,  $\psi = 0.6$  was defined and the first chain was initialized with  $\boldsymbol{\mu} = \frac{1}{5}$ , while the second was with  $\boldsymbol{\mu} = \frac{4}{5}$ . On the other hand, several models were generated for cases in which such a component was considered as a hyperparameter, taking into account a *grid* of nine equally spaced elements ranging from 0.1 to 0.9.

To summarize the resulting information, we calculated, for each parameter, the MAP estimate (Maximum a Posteriori). Thus, regarding the latent variables  $Z_l$ 's, we obtained the most frequent value, meaning the posterior mode.

### 3.2 Performance metrics

Let  $\tilde{\beta}_0(\cdot)$  be the simple functional mean obtained from the functional responses of  $m$  individuals so that  $\tilde{\beta}_0(t_{ij}) = \frac{1}{m} \sum_{i=1}^m y_i(t_{ij})$  is the value of this functional mean evaluated at point  $t_{ij}$ . Now define  $\hat{y}_{ij} = \hat{y}_i(t_{ij}) = \hat{\beta}_0(t_{ij}) + \sum_{l=1}^p x_{li} \hat{Z}_l \hat{\beta}_l(t_{ij})$  (see Expression 2 in Section 1 of the Supplementary Material) as the proposed model prediction of the  $i$ th functional response at the evaluation point  $t_{ij}$ , so then we have

$$1 - \frac{(\sum_{i=1}^m n_i - 1) \sum_{i=1}^m \sum_{j=1}^{n_i} (y_{ij} - \hat{y}_{ij})^2}{\left( \sum_{i=1}^m n_i - \sum_{l=1}^p I_{\{\hat{Z}_l > 0\}} K \right) \sum_{i=1}^m \sum_{j=1}^{n_i} (y_{ij} - \tilde{\beta}_0(t_{ij}))^2}, \quad (7)$$

as a goodness-of-fit performance metric for the functional context, being similar to the adjusted  $R^2$ . Thus, the closer the metric is to one, the better the performance. The  $\hat{Z}_l$ 's represent the most frequent values in the chain for each of the respective  $Z_l$ 's.

Comparisons and performance evaluations of results obtained from our numerical experiments were performed using the metric presented in the Expression (7) and the Mean Squared Error (MSE) defined as follows. Let  $g_i(t_{ij}) = \sum_{l=1}^p x_{li} Z_l \beta_l(t_{ij})$ , so that the model in (2) can also be written as  $y_{ij} = \beta_0(t_{ij}) + g_i(t_{ij}) + \epsilon_{ij}$ . In particular, in our numerical experiments,  $g_i(t_{ij}) = \beta_3(t_{ij})X_{3i} + \beta_5(t_{ij})X_{5i}$ . Thus, the MSE is calculated as follows:

$$\text{MSE} = \frac{1}{\sum_{i=1}^m n_i} \sum_{i=1}^m \sum_{j=1}^{n_i} [(\beta_0(t_{ij}) + g_i(t_{ij})) - (\hat{\beta}_0(t_{ij}) + \hat{g}_i(t_{ij}))]^2, \quad (8)$$

where  $\hat{g}_i(t_{ij}) = \sum_{l=1}^p x_{li} \hat{Z}_l \hat{\beta}_l(t_{ij})$ . Thus, the MSE evaluates the proximity between the true mean (expected) functional response curve,  $\beta_0(t_{ij}) + g_i(t_{ij})$ , and the estimated one,  $\hat{\beta}_0(t_{ij}) + \hat{g}_i(t_{ij})$ . It is worth noticing that as the points  $t_{ij}$ 's are equidistant in all curves, the MSE is proportional to the IMSE (Integrated Mean Square Error).

Table 1: Performance metrics (Eq. 7) of the proposed Bayesian approach with  $\mu$  as a hyperparameter and as a parameter, according to the different configurations of  $K$  B-spline basis functions, two dataset lengths ( $m \in \{10, 15\}$ ) and two noise variances,  $\sigma^2 = (0.2)^2$  and  $\sigma^2 = (20)^2$ .

$\sigma$	$m$	$K$	$\mu$ (Hyperparameter)								$\mu$ (Parameter)	
			0.1	0.2	0.3	0.4	0.5	0.6	0.7	0.8		0.9
0.2	10	5	0.99945	0.99946	0.99946	0.99947	0.99945	0.99945	0.99946	0.99945	0.99945	0.99947
		10	0.99993	0.99989	0.99987	0.99989	0.99990	0.99988	0.99991	0.99990	0.99992	0.99985
		15	0.99968	0.99976	0.99974	0.99951	0.99970	0.99971	0.99970	0.99965	0.99963	0.99957
	15	5	0.99920	0.99920	0.99920	0.99920	0.99920	0.99919	0.99919	0.99919	0.99919	0.99919
		10	0.99995	0.99994	0.99994	0.99995	0.99996	0.99995	0.99995	0.99995	0.99995	0.99995
		15	0.99990	0.99990	0.99983	0.99986	0.99988	0.99991	0.99983	0.99990	0.99992	0.99990
20	10	5	0.81410	0.81418	0.81381	0.81367	0.81343	0.81447	0.81391	0.81222	0.81485	0.81333
		10	0.80982	0.81346	0.81047	0.81186	0.81342	0.81209	0.80735	0.81158	0.81121	0.81316
		15	0.80450	0.81138	0.81028	0.80865	0.80474	0.81268	0.80949	0.80975	0.80985	0.81112
	15	5	0.75635	0.75703	0.75558	0.76183	0.76300	0.76284	0.76297	0.76271	0.76340	0.75593
		10	0.75773	0.75707	0.75726	0.75795	0.75770	0.75702	0.75774	0.75737	0.76165	0.75748
		15	0.75626	0.75634	0.75537	0.75601	0.75300	0.75771	0.75456	0.75414	0.75423	0.75782

### 3.3 Results

This section exhibits the results of two different types of numerical experiments. Firstly, the proposed method is tested with synthetic data without replications. Secondly, simulations show the performance of the procedure under a scheme with replications. The diagnostic analysis based on the method proposed by Gelman and Rubin (1992) attested the convergence of the chains of the partial functional coefficients in all experiments and in all model configurations evaluated after the *burn-in* period. It is also important to notice that B-splines were used for the basis expansion of all partial functional coefficients.

#### 3.3.1 Studies with Synthetic Data

Four synthetic data sets were generated for this study as described in Section 3.1. Two sets with a low level of dispersion ( $\sigma = 0.2$ ), one with  $m = 10$  curves and another with  $m = 15$  curves, and the other two sets with a higher level of dispersion ( $\sigma = 20$ ), one with  $m = 10$  curves and one with  $m = 15$  curves. Three possible values for  $K$  ( $K \in \{5, 10, 15\}$ ) were tested for each of these data sets, which represents the total number of basis functions used in the expansion of each partial functional coefficient. The model which considers the  $\mu$  component as a parameter was evaluated, as well as the model that considers  $\mu$  as a hyperparameter, in which case the search grid is  $\{0.1, 0.2, 0.3, 0.4, 0.5, 0.6, 0.7, 0.8, 0.9\}$ .

Table 1 presents the performance metrics calculated following the Expression (7) for the various proposed model configurations. The highlighted cells in the table indicate the best model configuration among those whose  $\mu$  is taken as a hyperparameter. According to the metric (7), the model explains almost all of the variability of the data generated with  $\sigma = 0.2$ . At the same time, it can explain more than 75% of the total variability when  $\sigma = 20$ . A relevant aspect is that the model configurations considering  $\mu$  as a parameter obtained very similar performance to the cases with  $\mu$  as a hyperparameter.



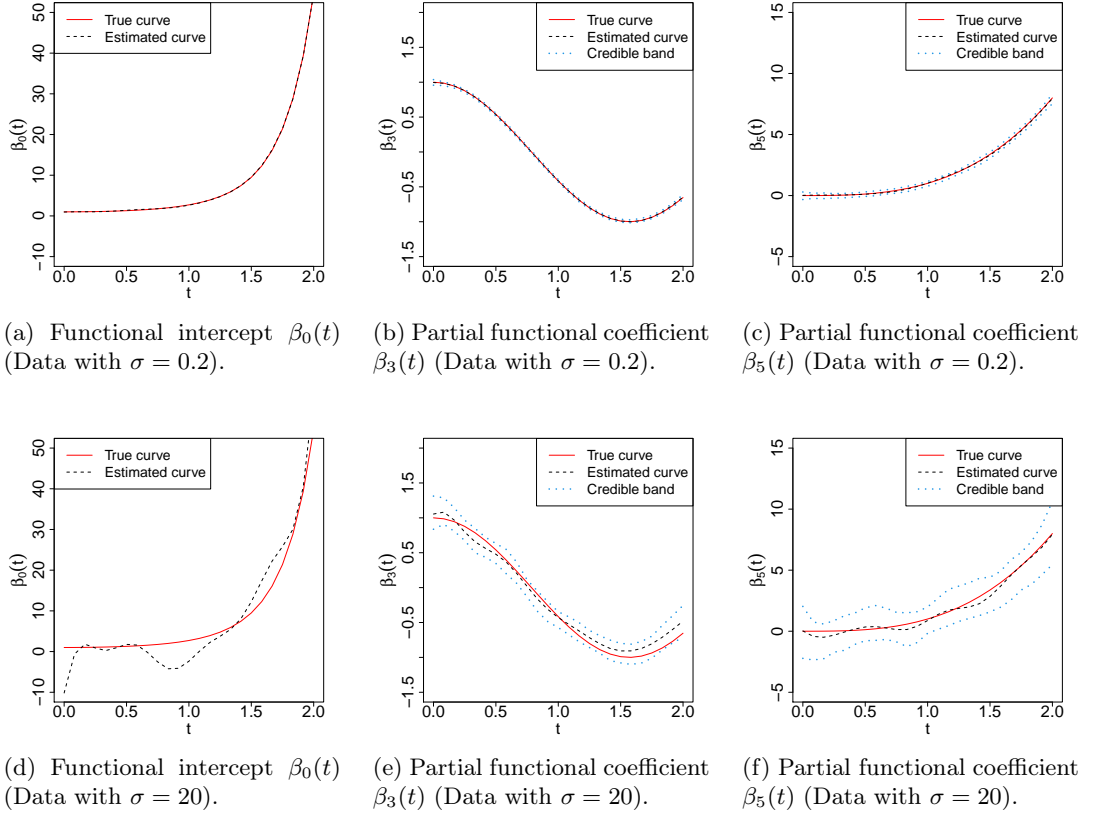


Figure 1: Intercept and partial functional coefficients (true and estimated) that were selected by the model, according to the data dispersion degree (configurations with  $K = 10$  and  $\mu = 0.1$  for the two levels of dispersion). 95% credible bands are also shown for the partial functional coefficients.

When assessing the results in Table 1, there is evidence that the proposed model has a low sensitivity in relation to the possible values that the hyperparameter  $\mu$  can assume, regardless of the degree of data dispersion ( $\sigma$ ), the number of curves ( $m$ ) and the number of bases ( $K$ ) used in the expansion of the partial functional coefficients. This low sensitivity to the hyperparameter value is a desired property, but it should be checked with more caution in a study with replications, as it is presented in Section 3.3.2.

Supplementary Table 1 displays the Mean Squared Error (MSE) as in (8) of the respective model settings. The best model for small variance ( $\sigma = 0.2$ ) gives an MSE of the order  $10^{-2}$ , while the MSE for  $\sigma = 20$  is of the order  $10^{-1}$ . As expected, the ability of the model to estimate the mean functional response in the study with a large  $\sigma$  is lower than in the study with a small  $\sigma$ . Finally, by comparing the MSEs it is possible to identify that the model performed predominantly better with data with  $m = 15$  than with data with ten curves ( $m = 10$ ).

As an example, Figure 1 presents the estimates  $\hat{\beta}_l(\cdot)$ 's of the partial functional coefficients selected by the model (data with  $m = 10$  and configurations with  $K = 10$  and  $\mu = 0.1$  for the two dispersion levels) and the estimates of the functional intercept  $\hat{\beta}_0(\cdot)$ . Figure 1 also shows the 95% credible bands for the functional coefficients the model selected. We computed these bands as follows. First, the two hundred vectors of parameters sampled by the Gibbs sampler were taken to construct the bands. Then the curves of the

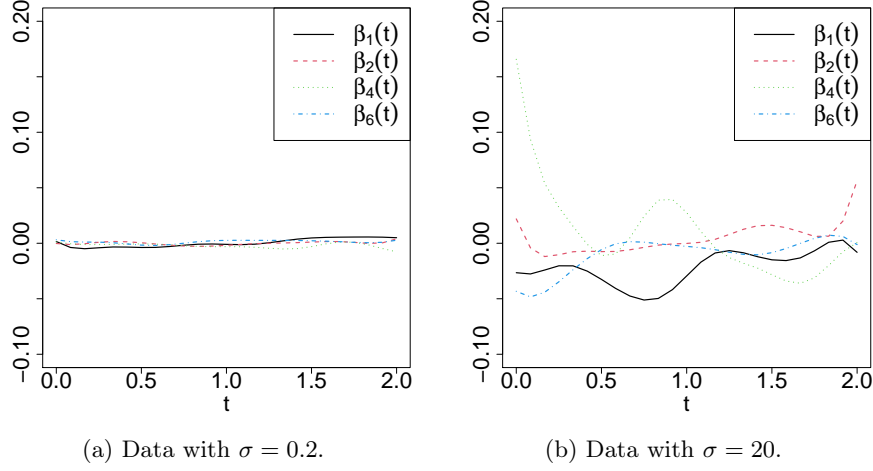


Figure 2: Partial estimated functional coefficients that were excluded by the model, according to the data dispersion degree.

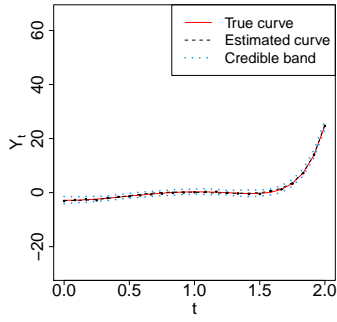
functional coefficients were generated through each of these vectors, totalling two hundred curves per functional coefficient. With this, by fixing  $t$ , it is possible to calculate the necessary quantiles for the construction of the credible bands since there are two hundred possible points for each functional coefficient and each  $t$ . The quantiles used to define the lower and upper bands were 2.5% and 97.5%.

The first relevant fact to be highlighted in Figure 1 is the ability of the model to exactly select the covariates that were used in the generation of synthetic data when using the configuration with  $K = 10$  and  $\mu = 0.1$ . Observing the posterior samples of each  $Z_l$  (not shown here), it is also verified that there was perfect agreement between the sampling points and the real values of the latent variables, meaning that a sample was obtained with all quantities equal to one for the cases in which  $Z_l = 1$  in the synthetic data, as well as a sample with all quantities equal to zero for the cases in which  $Z_l = 0$ . This is seen in both data dispersion scenarios ( $\sigma = 0.2$  and  $\sigma = 20$ ).

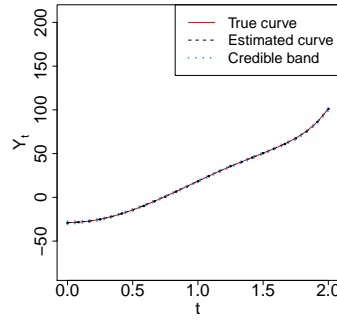
The model's ability to select the covariates used in the synthetic data generation remains high with other  $K$  and  $\mu$  configurations. This property will be further investigated in the study with replications presented in Section 3.3.2. A high fitting capacity is also observed in Figure 1, mainly in the scenario with low dispersion data. The true and estimated curves overlap, making it impossible to distinguish them only by graphic visualization. The estimation naturally loses precision when considering data with a higher noise level, but the model still provides satisfactory estimates.

Although only the functional coefficients  $Z_3\beta_3(t)$  and  $Z_5\beta_5(t)$  are different from zero, since  $\hat{Z}_3$  and  $\hat{Z}_5$  are equal to one, the proposed model still provides the estimates of the other  $\beta_l(t)$ 's, even if the latent variables nullify such estimates. Figure 2 presents the estimates of all other partial functional coefficients associated with the covariates excluded from the model. All the functional estimates in Figure 2 are around zero, regardless of the degree of dispersion of the synthetic data used. This pattern for the partial functional coefficients of the excluded covariates is expected due to the very characterization of the full conditional distributions of the basis expansion coefficients (the  $b$ 's) as a function of the respective latent variables.

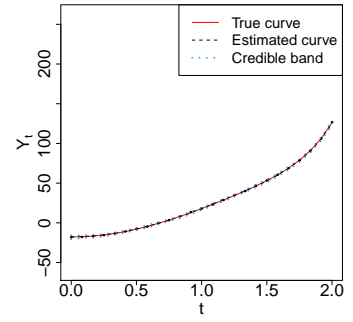
To conclude the study of this section, Figure 3 presents the first three mean (or ex-



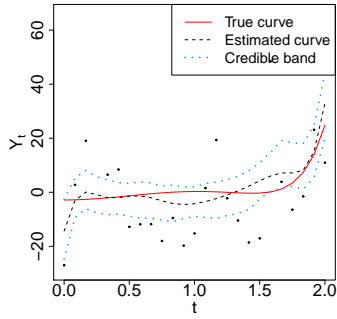
(a) 1<sup>st</sup> functional response (Data with  $\sigma = 0.2$ ).



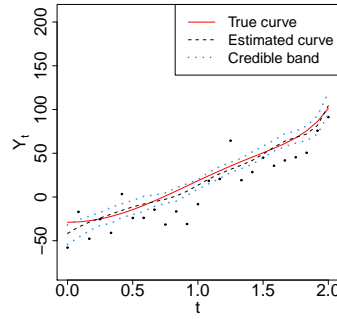
(b) 2<sup>nd</sup> functional response (Data with  $\sigma = 0.2$ ).



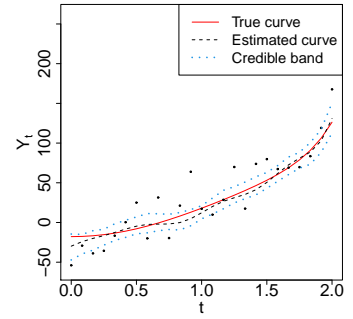
(c) 3<sup>rd</sup> functional response (Data with  $\sigma = 0.2$ ).



(d) 1<sup>st</sup> functional response (Data with  $\sigma = 20$ ).



(e) 2<sup>nd</sup> functional response (Data with  $\sigma = 20$ ).



(f) 3<sup>rd</sup> functional response (Data with  $\sigma = 20$ ).

Figure 3: Data and mean functional responses,  $\beta_0(t_{ij}) + g_i(t_{ij})$ , for  $i = 1, 2, 3$  and  $j = 1 \dots, 25$  (true and estimated along with credible bands), according to the data dispersion degree.

pected) functional response curves (among the total of  $m = 10$ ), together with the respective observed data and the respective estimated curves for each data dispersion level. In addition, credible bands for the respective mean functional responses are also presented. The bands are generated similarly to those obtained for the functional coefficients in Figure 1. More specifically, from the two hundred parameter vectors sampled by the Gibbs sampler, the estimated mean functional response curves corresponding to each of those vectors were generated, totalling two hundred curves per functional response. From there, the 2.5% and 97.5% quantiles are calculated as previously described and used to define the lower and upper bands.

### 3.3.2 Simulations

In this section, we conducted a study with replications to obtain more consistent conclusions regarding our proposed methodology’s fit performance and model selection capacity. In addition, the sensitivity of the proposed model to the hyperparameter  $\mu$  is also investigated. The synthetic data of each replication contains  $m = 10$  curves generated as described in Section 3.1 with  $K = 10$  B-spline basis functions considered for the expansion of the functional coefficients.

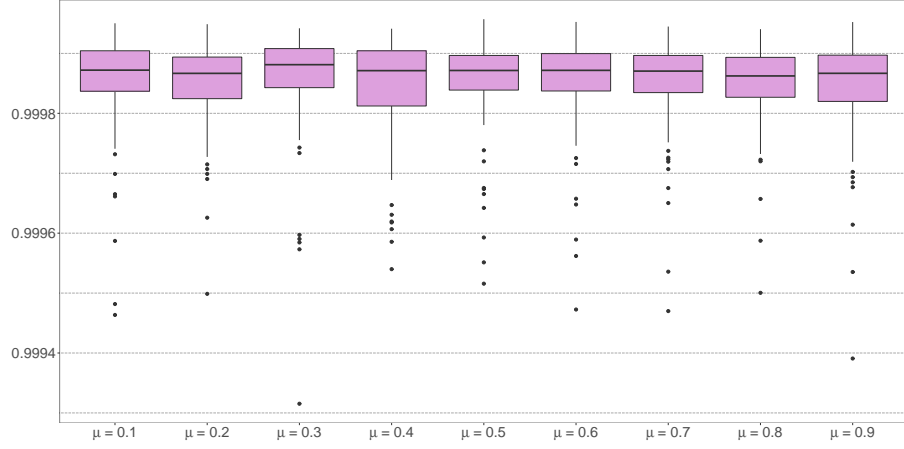
We conducted our simulations considering two dispersion levels for the data ( $\sigma = 0.2$  and  $\sigma = 20$ ). Thus, ten model configurations were tested under each dispersion scenario, nine of which consider  $\mu$  as a hyperparameter and one that considers it as a parameter. In all model configurations, regardless of the dispersion scenario, a total of one hundred replications were used.

Figure 4 shows the boxplots for metric (7) for each tested model configuration in our simulations. It is noticed that the proposed model, regardless of the dispersion scenario, has a low sensitivity to the hyperparameter  $\mu$ . This property guarantees that the model can smooth and select the partial functional coefficients (and consequently the covariates), regardless of the prior choice for  $\mu$ . Supplementary Figure 1 presents the MSE boxplots for each tested model configuration. It is also possible to conclude the low sensitivity of the proposed model to the choice of the hyperparameter  $\mu$ . Both metrics show an expected behavior concerning  $\sigma$  since the performance of the models is better when the data present low dispersion ( $\sigma = 0.2$ ). It is also worth mentioning that both metrics are well-behaved because there is symmetry and a few discrepant values in the boxplots.

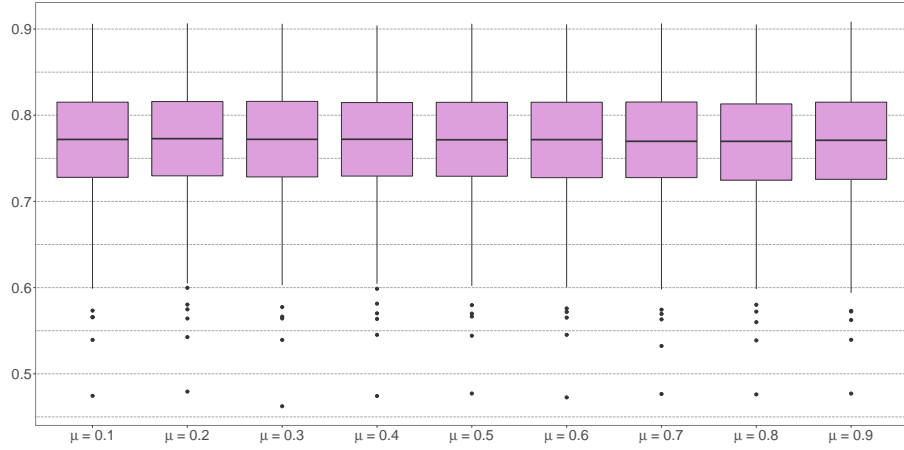
We also conducted simulations to evaluate the model’s performance considering  $\mu$  as a parameter. Supplementary Figure 2 shows the boxplots of the metric (7) according to the data dispersion level. Similarly, Supplementary Figure 3 presents the boxplots of the MSEs. For both data dispersion levels and regardless of the metric being analyzed, it is clear that the model configuration with  $\mu$  as a parameter is as efficient as the other configurations in terms of goodness of fit and estimation quality.

In addition to the goodness of fit, it is also interesting to assess the variable selection ability for each model configuration among the one hundred replications. Table 2 presents the proportion among the 100 replications that each functional coefficient estimate ( $\hat{Z}_l \hat{\beta}_l(\cdot)$ , for  $l = 1, \dots, 6$ ) was different from zero. For data with a low dispersion level ( $\sigma = 0.2$ ), we can observe in Table 2 that all tested model configurations correctly performed the selection in all replications. However, the selection for the data with a higher dispersion level ( $\sigma = 20$ ) is not perfect in all replications, although it remains highly accurate.

Table 2 shows that except for configurations with  $\mu$  as a parameter and as hyperparameter with  $\mu = 0.1$  when  $\sigma = 20$ , all other configurations (for both  $\sigma = 0.2$  and  $\sigma = 20$ ) correctly selected the covariates associated with the partial functional coefficients  $\hat{\beta}_3(\cdot)$  and  $\hat{\beta}_5(\cdot)$  in all replications, allowing us to conclude that the model has no difficulty in



(a) Data with  $\sigma = 0.2$ .



(b) Data with  $\sigma = 20$ .

Figure 4: Boxplots of the metric (7) for the various model configurations tested when  $\mu$  is a hyperparameter, according to the data dispersion degree.

Table 2: Proportions of non-zero estimated functional coefficients among the 100 replications for the various model configurations tested ( $\mu$  as a parameter or hyperparameter), according to the data dispersion degree ( $\sigma = 0.2$  and  $\sigma = 20$ ).

$\sigma$	$\hat{Z}_l \hat{\beta}_l(\cdot)$	$\mu$ (Hyperparameter)									$\mu$ (Parameter)
		0.1	0.2	0.3	0.4	0.5	0.6	0.7	0.8	0.9	
0.2	$\hat{Z}_1 \hat{\beta}_1(\cdot)$	0	0	0	0	0	0	0	0	0	0
	$\hat{Z}_2 \hat{\beta}_2(\cdot)$	0	0	0	0	0	0	0	0	0	0
	$\hat{Z}_3 \hat{\beta}_3(\cdot)$	1	1	1	1	1	1	1	1	1	1
	$\hat{Z}_4 \hat{\beta}_4(\cdot)$	0	0	0	0	0	0	0	0	0	0
	$\hat{Z}_5 \hat{\beta}_5(\cdot)$	1	1	1	1	1	1	1	1	1	1
	$\hat{Z}_6 \hat{\beta}_6(\cdot)$	0	0	0	0	0	0	0	0	0	0
20	$\hat{Z}_1 \hat{\beta}_1(\cdot)$	0.01	0.03	0.03	0.04	0.04	0.04	0.05	0.05	0.13	0.01
	$\hat{Z}_2 \hat{\beta}_2(\cdot)$	0.01	0.02	0.02	0.02	0.02	0.02	0.05	0.07	0.12	0.01
	$\hat{Z}_3 \hat{\beta}_3(\cdot)$	1	1	1	1	1	1	1	1	1	1
	$\hat{Z}_4 \hat{\beta}_4(\cdot)$	0	0	0.01	0.01	0.02	0.02	0.02	0.04	0.09	0
	$\hat{Z}_5 \hat{\beta}_5(\cdot)$	0.99	1	1	1	1	1	1	1	1	0.99
	$\hat{Z}_6 \hat{\beta}_6(\cdot)$	0.03	0.03	0.03	0.04	0.03	0.04	0.04	0.05	0.09	0.03

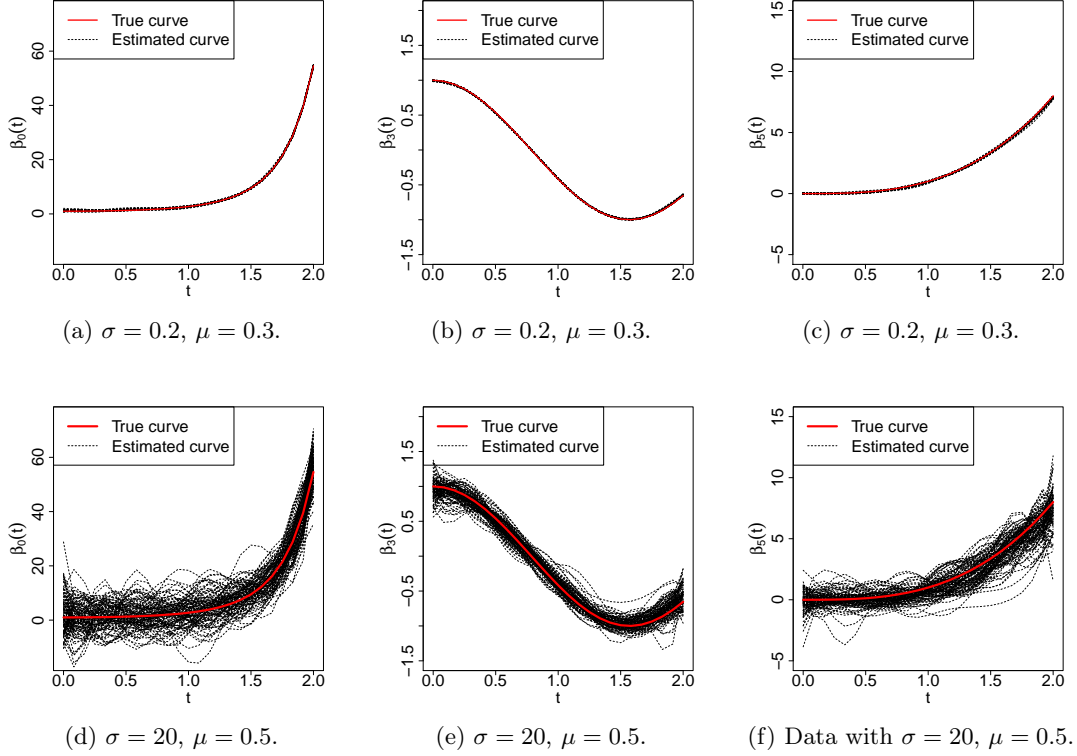


Figure 5: Intercept and partial functional coefficients (3<sup>rd</sup> and 5<sup>th</sup>, true in red and estimated for the replications in which the coefficients were selected in black) from the model that considers  $\mu$  as a hyperparameter (top row  $\mu = 0.3$ , bottom row  $\mu = 0.5$ ), according to the data dispersion degree (top row  $\sigma = 0.2$ , bottom row  $\sigma = 20$ ).

selecting the partial functional coefficients that should remain in the functional regression. Furthermore, we can see that most of the selection errors committed in the scenario with  $\sigma = 20$  happened when the model fails to exclude a coefficient that should be excluded. The proportions associated with the coefficients that should be excluded from the regression are generally below 7%. However, it is worth noting that slightly higher proportions were observed for the configuration that considers  $\mu = 0.9$ .

Figure 5 shows the estimates of the partial functional coefficients that the proposed model predominantly selected ( $\hat{\beta}_3(\cdot)$  and  $\hat{\beta}_5(\cdot)$ ), as well as the estimates obtained in each replication for the functional intercept. The results in this figure correspond to the model that considers  $\mu$  as a hyperparameter with a specific value of  $\mu$  for each data dispersion level. We chose  $\mu$  for each dispersion level as the value that resulted in the highest mean value of the performance metric in (7) over the one hundred replications. Thus, the model with  $\mu = 0.3$  was used for data with  $\sigma = 0.2$  and the model with  $\mu = 0.5$  for data with  $\sigma = 20$ . When analyzing the intercept and partial functional coefficient results, we notice that the curves almost perfectly overlap in the scenario considering the data with low dispersion ( $\sigma = 0.2$ ), even when plotting one hundred estimates. On the other hand, the estimated curves for the scenario with large dispersion ( $\sigma = 20$ ) are more dispersed but follow the same trend.

Similarly, Supplementary Figure 4 shows the estimated partial functional coefficients ( $\hat{\beta}_3(\cdot)$  and  $\hat{\beta}_5(\cdot)$ ) and functional intercept for the case when the model considers  $\mu$  as a

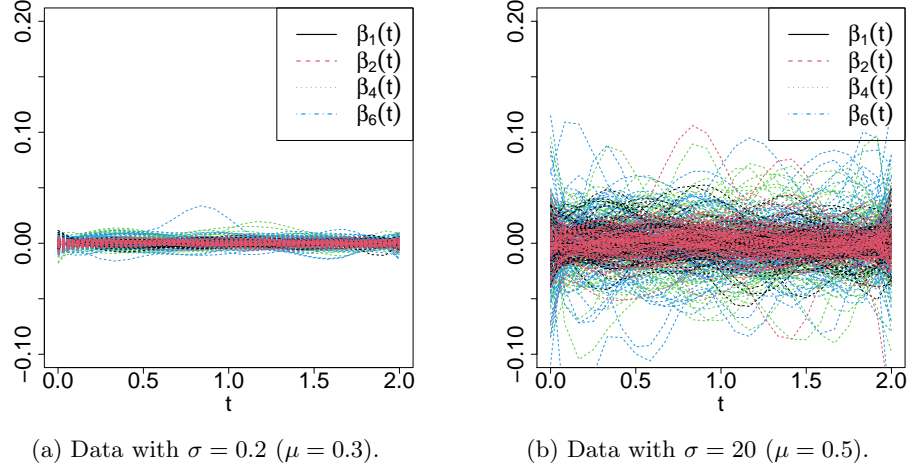


Figure 6: Estimated partial functional coefficients (1<sup>st</sup>, 2<sup>nd</sup>, 4<sup>th</sup> and 6<sup>th</sup>) from the model that considers  $\mu$  as a hyperparameter, according to the data dispersion degree, for the replications whose coefficients were excluded among the total of 100 replications.

parameter. The conclusions are similar to the ones obtained from Figure 5, showing that the version with more layers in the hierarchical model does not significantly differ from the version which considers  $\mu$  fixed.

To complement the analysis of the proposed methodology through simulations, Figure 6 presents the estimates of all the other partial functional coefficients ( $\hat{\beta}_1(\cdot)$ ,  $\hat{\beta}_2(\cdot)$ ,  $\hat{\beta}_4(\cdot)$  and  $\hat{\beta}_6(\cdot)$ ) from the model that considers  $\mu$  as a hyperparameter that are associated with the excluded variables, according to the data dispersion degree (Supplementary Figure 5 presents the corresponding plots obtained by the model that considers  $\mu$  as a parameter). Regardless of the data dispersion degree and the approach to  $\mu$ , Figure 6 and Supplementary Figure 5 shows that all the functional estimates in question are around zero.

### 3.4 grLASSO, grSCAD and grMCP versus proposed model

As emphasized in Section 2, there are some methods that can compete with the method proposed in this paper for variable selection in FOSR. Through basis expansion of the functional coefficients, FOSR can be dealt with as a conventional regression problem, thus enabling the use of techniques developed for cross-sectional data. A relevant fact is that as the coefficients are expanded through basis functions, the characterization of each functional coefficient ( $\beta_l(\cdot)$ ) is determined by a distinct group of scalar coefficients ( $b_{l,i}$ 's) from the basis expansion.

Among the methods that can be applied in this context of FOSR with functional coefficients expanded via basis functions, we can highlight LASSO (Least Absolute Shrinkage and Selection Operator) (Tibshirani, 1996), SCAD (Smoothly Clipped Absolute Deviation) penalized regression (Fan and Li, 2001) and MCP (Minimax Concave Penalty) penalized regression (Zhang, 2010), which are regularization and variable selection methods for regression analysis. However, when any of these methods are applied to functional regression after the basis expansion of the functional coefficients, the variable selection is not guaranteed since the method will not consider the existence of groups among the scalar coefficients derived from the basis expansions. In other words, selection of some of the expansion bases may occur; however, not of the variables, since for that, it would be necessary to zero

the functional coefficients as a whole, which would mean to zero together all the scalar coefficients of the expansion of the respective functional coefficient.

Naturally, when applying a procedure that takes into account the structure in groups in order to simultaneously include or exclude the groups of these scalar coefficients, one truly has a variable selection mechanism for the aforementioned functional structure. Fortunately, one can find papers in the literature of linear models that extend the ideas of Tibshirani (1996), Fan and Li (2001) and Zhang (2010) for the context of selecting groups of variables. First, Yuan and Lin (2006) proposed *group LASSO* (grLASSO), which performs this type of group selection, and then Wang et al. (2007) proposed a group selection method which uses the SCAD penalty (grSCAD), while Huang et al. (2012) showed something similar for the MCP penalty (grMCP).

Thus, the regularization and selection methods in groups described above (grLASSO, grSCAD and grMCP) are considered in this section to carry out a comparative analysis with our proposed method in regards to the fit quality and the correct selection capacity of the variables in each one of the methods in question. We used synthetic data replications generated as described in Section 3.1 with  $m = 10$  curves and  $K = 10$  B-spline bases for each functional coefficient in each replication. Finally, it is worth noting that the models are compared in two scenarios, one with low dispersion data ( $\sigma = 0.2$ ) and another with higher dispersion data ( $\sigma = 20$ ), and 100 replications were used in each of these scenarios.

The **grpreg** function from the *grpreg* package (Breheny et al., 2021) of the statistical software R was used to obtain the results of the grLASSO, grSCAD and grMCP models. For the implementation of the estimation algorithm of the aforementioned methods, the **grpreg** function refers to the works presented in Breheny and Huang (2013) and Huang et al. (2012).

For the correct implementation of FOSR through the **grpreg** function, it is necessary to assign the vector  $\tilde{\mathbf{y}}_{..} = (\tilde{\mathbf{y}}_{1.}', \tilde{\mathbf{y}}_{2.}', \dots, \tilde{\mathbf{y}}_{m.}')'$  (in which each  $\tilde{\mathbf{y}}_{i.} = (\tilde{y}_{i1}, \tilde{y}_{i2}, \dots, \tilde{y}_{in_i})'$ ) as the response vector, while for the design matrix considering  $n_i = n$ ,  $\forall i \in \{1, 2, \dots, m\}$ , one should use the matrix resulting from the Kronecker product between  $(\mathbf{X}_{p \times m})'$  (the matrix formed by  $x_{li}$ 's) and  $\mathbf{B}_{n \times K}$  (the matrix of basis function evaluations), that is

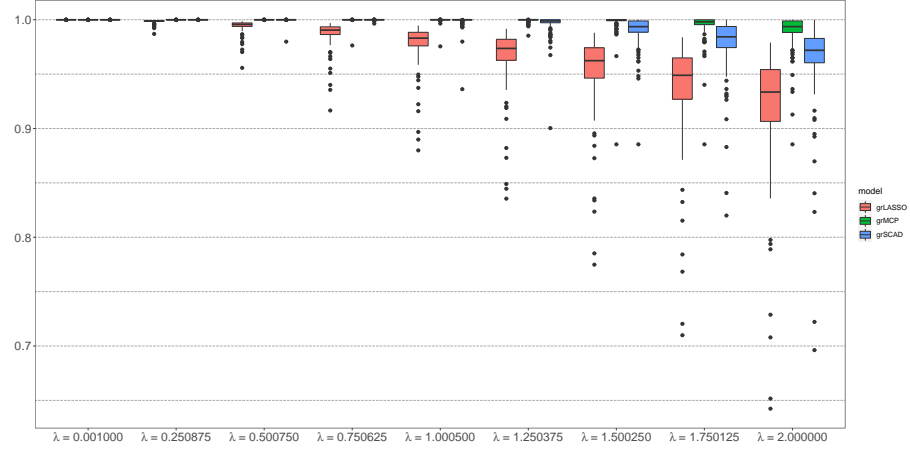
$$(\mathbf{X}_{p \times m})' \otimes \mathbf{B}_{n \times K} = \begin{bmatrix} x_{11}\mathbf{B} & \dots & x_{p1}\mathbf{B} \\ \vdots & \dots & \vdots \\ x_{1m}\mathbf{B} & \dots & x_{pm}\mathbf{B} \end{bmatrix}.$$

For the *group* argument of the **grpreg** function, one must define a vector that describes the grouping of the coefficients, whereas, for the *penalty* argument, one can select either “grLASSO,” “grSCAD” or “grMCP” expression to define the model to be used.

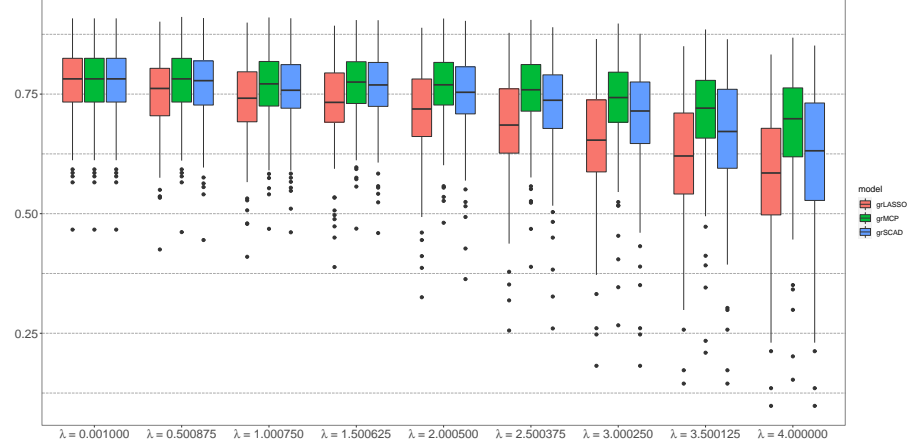
Finally, the **grpreg** function requires the definition of a search grid for the regularization parameter  $\lambda$  or the definition of a single value for it. Thus, in this work, we chose to define a single  $\lambda$  value within the function at a time. However, we ran the function for different values of  $\lambda$  defined over a *grid* characterized by a sequence that was generated in R as follows: `seq(0.001, 2, length = 9)` for  $\sigma = 0.2$ , and `seq(0.001, 4, length = 9)` for  $\sigma = 20$ . Both sequences have the same length, but different upper bounds (2 and 4), from which points we can observe that the regularization in data with greater dispersion becomes too intense. Thus, for each data dispersion level, each  $\lambda$  value of the respective sequence, and each of the hundred replications, the **grpreg** function was applied, and the performance metrics were subsequently calculated.

Figure 7 and Supplementary Figure 6 present the boxplots of the metric (7) and MSE, respectively, for each competing model according to the data dispersion degree and the respective  $\lambda$  values tested. Regardless of which metric is evaluated (metric (7) or MSE),





(a) Data with  $\sigma = 0.2$ .



(b) Data with  $\sigma = 20$ .

Figure 7: Boxplots of the metric (7) for each competing model (grLASSO, grSCAD and grMCP), according to the data dispersion degree and the respective regularization  $\lambda$  values tested.

Table 3: Proportion of non-zero estimates for each functional coefficient among the 100 replications, according to each model configuration tested. Data with  $\sigma = 0.2$ .

Model	$\hat{\beta}_l(.)$	$\lambda$								
		0.001	0.250875	0.50075	0.750625	1.0005	1.250375	1.50025	1.750125	2
grLASSO	$\hat{\beta}_1(.)$	1	0.02	0.01	0.01	0.01	0.01	0.01	0.01	0.01
	$\hat{\beta}_2(.)$	1	0.02	0.02	0.02	0.02	0.02	0.02	0.02	0.02
	$\hat{\beta}_3(.)$	1	1	1	1	1	1	1	1	1
	$\hat{\beta}_4(.)$	1	0.05	0.05	0.05	0.05	0.03	0.03	0.02	0.02
	$\hat{\beta}_5(.)$	1	1	1	1	1	1	0.99	0.97	0.96
	$\hat{\beta}_6(.)$	1	0.09	0.07	0.06	0.04	0.04	0.04	0.04	0.03
grMCP	$\hat{\beta}_1(.)$	1	0	0	0	0	0	0	0	0
	$\hat{\beta}_2(.)$	1	0	0	0.01	0.01	0	0	0	0
	$\hat{\beta}_3(.)$	1	1	1	1	1	1	1	1	1
	$\hat{\beta}_4(.)$	1	0	0	0.01	0.01	0	0	0	0
	$\hat{\beta}_5(.)$	1	1	1	0.99	0.99	1	0.99	0.99	0.97
	$\hat{\beta}_6(.)$	1	0	0	0	0	0	0	0	0
grSCAD	$\hat{\beta}_1(.)$	1	0	0	0	0	0	0	0	0
	$\hat{\beta}_2(.)$	1	0	0.01	0	0	0	0	0	0
	$\hat{\beta}_3(.)$	1	1	1	1	1	1	1	1	1
	$\hat{\beta}_4(.)$	1	0	0.01	0	0	0	0	0	0
	$\hat{\beta}_5(.)$	1	1	1	1	1	1	0.99	0.99	0.97
	$\hat{\beta}_6(.)$	1	0	0	0	0	0	0	0	0

we can observe that the quality of the fit starts to decrease from a certain  $\lambda$  value, indicating that the regularization becomes more and more intense and farther from the ideal if large values of  $\lambda$  are used. This discrepancy is even more evident in the scenario with low data dispersion since the boxplots for low values of the regularization parameter are at a level very close to the perfect value (1 for the metric (7) and 0 for the MSE), so close that it is even difficult to visualize them in the figures, while the boxplots associated with the high values of  $\lambda$  are at much worse levels of the performance metrics and with larger interquartile ranges. Figure 8 and Supplementary Figure 7 present a comparison between our proposed model and the competing grLASSO, grMCP and grSCAD methods regarding the metric (7) and MSE, respectively.

In order to demonstrate the capacity of each competing model to select the correct covariates across different values of  $\lambda$  and dispersion levels, Tables 3 and 4 present the proportion of times that each functional coefficient estimate was different from zero among the total of 100 replications. We notice that no model could perform the variable selection for the lowest regularization level ( $\lambda = 0.001$ ) for all three competing methods (all proportions were equal to one). For the other  $\lambda$  values tested, the models started to select the variables. Such selection for data with low dispersion is predominantly correct from  $\lambda = 0.250875$ , while for data with large dispersion from  $\lambda = 2.005$ . However, the non-zero proportions in Table 4 associated with the fifth functional coefficient become lower for larger values of  $\lambda$ .

It is noted (Table 4 and Supplementary Figure 6(b)) that the competing models are not able to balance very well the accuracy in the selection in the scenario with greater data dispersion while preserving the quality of the fit according to the metrics under study, meaning that they need to lose fit quality and increase the regularization to gain better accuracy in the selection.

For last finding that can be obtained when evaluating Tables 3 and 4 is that the grSCAD and grMCP models stand out from the grLASSO model in the scenario with low data dispersion ( $\sigma = 0.2$ ), better selecting the variables for the different  $\lambda$  values tested.

Table 4: Proportion of non-zero estimates for each functional coefficient among the 100 replications, according to each model configuration tested. Data with  $\sigma = 20$ .

Model	$\hat{\beta}_l(\cdot)$	$\lambda$								
		0.001	0.500875	1.00075	1.500625	2.0005	2.500375	3.00025	3.500125	4
grLASSO	$\hat{\beta}_1(\cdot)$	1	0.94	0.62	0.2	0.08	0.04	0.03	0.03	0.01
	$\hat{\beta}_2(\cdot)$	1	0.97	0.67	0.17	0.05	0.04	0.01	0	0
	$\hat{\beta}_3(\cdot)$	1	1	1	1	1	1	1	1	1
	$\hat{\beta}_4(\cdot)$	1	0.97	0.76	0.27	0.09	0.04	0.04	0.03	0.02
	$\hat{\beta}_5(\cdot)$	1	1	1	0.98	0.96	0.9	0.88	0.75	0.63
	$\hat{\beta}_6(\cdot)$	1	0.99	0.6	0.2	0.1	0.07	0.05	0.03	0.03
grMCP	$\hat{\beta}_1(\cdot)$	1	0.95	0.43	0.1	0.01	0	0	0	0
	$\hat{\beta}_2(\cdot)$	1	0.96	0.47	0.04	0	0	0	0	0
	$\hat{\beta}_3(\cdot)$	1	1	1	1	1	1	1	1	1
	$\hat{\beta}_4(\cdot)$	1	0.94	0.53	0.08	0.01	0	0	0	0
	$\hat{\beta}_5(\cdot)$	1	1	0.98	1	0.98	0.92	0.84	0.74	0.54
	$\hat{\beta}_6(\cdot)$	1	1	0.49	0.04	0	0	0	0	0
grSCAD	$\hat{\beta}_1(\cdot)$	1	0.95	0.48	0.11	0.03	0.02	0	0	0
	$\hat{\beta}_2(\cdot)$	1	0.92	0.55	0.07	0.01	0.01	0.01	0	0
	$\hat{\beta}_3(\cdot)$	1	1	1	1	1	1	1	1	1
	$\hat{\beta}_4(\cdot)$	1	0.94	0.56	0.12	0	0	0.01	0.01	0.01
	$\hat{\beta}_5(\cdot)$	1	1	1	1	0.97	0.91	0.85	0.73	0.59
	$\hat{\beta}_6(\cdot)$	1	0.96	0.55	0.09	0.03	0.02	0.01	0.01	0.01

Table 5: Proportion of non-zero estimates for each functional coefficient among the 100 replications, according to the best tested model configuration. Data with  $\sigma = 0.2$ .

$Z_l \hat{\beta}_l(\cdot)$ (proposed model) or $\hat{\beta}_l(\cdot)$ (adversary models)	Proposed model ( $\mu = 0.3$ and $\lambda = \sqrt{2}$ )	Proposed model ( $\mu$ as a parameter and $\lambda = \sqrt{2}$ )	grLASSO ( $\lambda = 0.001$ )	grMCP ( $\lambda = 0.250875$ )	grSCAD ( $\lambda = 0.250875$ )
1 <sup>st</sup> functional coefficient	0	0	1	0	0
2 <sup>nd</sup> functional coefficient	0	0	1	0	0
3 <sup>rd</sup> functional coefficient	1	1	1	1	1
4 <sup>th</sup> functional coefficient	0	0	1	0	0
5 <sup>th</sup> functional coefficient	1	1	1	1	1
6 <sup>th</sup> functional coefficient	0	0	1	0	0

Tables 5 and 6 allow a brief comparison regarding the capacity to select the correct covariates among the best configurations tested for the competing models, as well as for our proposed model. The best model configuration was chosen according to the performance metric (7). For this, the average metric value over the one hundred replications was calculated for each model configuration, and we then selected the model with the configuration that returned the highest of these averages.

For comparisons between models in this section, specifically in relation to our proposed model, the results obtained for the simulation study presented in Subsection 3.3.2 were used. As seen in Subsection 3.3.2, the proposed model has a low sensitivity to the hyperparameter  $\mu$ , which is desired for conventional hyperparameters. On the other hand, it is natural that the model has some sensitivity to the hyperparameter  $\lambda$  since this is the only hyperparameter that truly plays the role of regularizer ( $\lambda$  is the a priori hyperparameter of the  $\tau_{ki}^2$ 's, presented in (3) and (4)). For the proposed model to not be at a disadvantage in this comparison, the ideal would be to test more  $\lambda$  values, as was done for the opponents. However, only the  $\lambda = \sqrt{2}$  value was tested due to the high computational cost demanded by applying the model on one hundred replications and several model configurations for  $\lambda$ . Even so, the proposed model with  $\lambda = \sqrt{2}$  presented great performance compared to the

Table 6: Proportion of non-zero estimates for each functional coefficient among the 100 replications, according to the best tested model configuration. Data with  $\sigma = 20$ .

$Z_l \hat{\beta}_l(\cdot)$ (proposed model) or $\hat{\beta}_l(\cdot)$ (adversary models)	Proposed model ( $\mu = 0.5$ and $\lambda = \sqrt{2}$ )	Proposed model ( $\mu$ as a parameter and $\lambda = \sqrt{2}$ )	grLASSO ( $\lambda = 0.001$ )	grMCP ( $\lambda = 0.500875$ )	grSCAD ( $\lambda = 0.001$ )
1 <sup>st</sup> functional coefficient	0.04	0.01	1	0.95	1
2 <sup>nd</sup> functional coefficient	0.02	0.01	1	0.96	1
3 <sup>rd</sup> functional coefficient	1	1	1	1	1
4 <sup>th</sup> functional coefficient	0.02	0	1	0.94	1
5 <sup>th</sup> functional coefficient	1	0.99	1	1	1
6 <sup>th</sup> functional coefficient	0.03	0.03	1	1	1

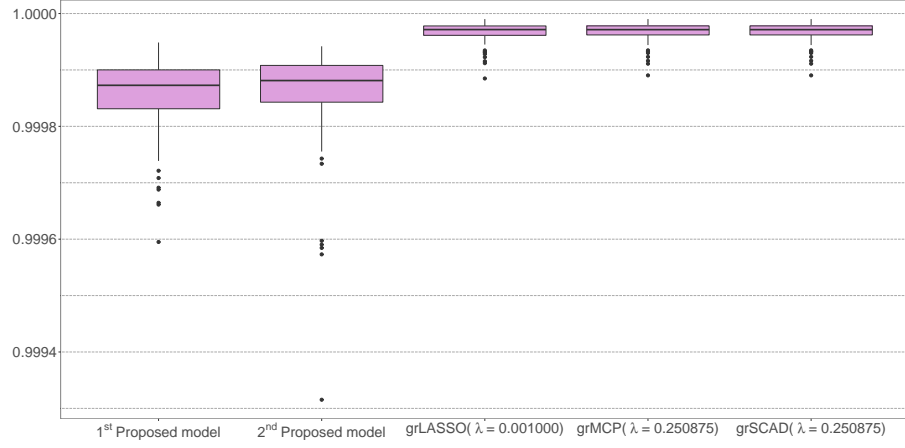
others, with excellent fit capacity and standing out even more in the accuracy regarding the selection of covariates.

The results presented in Table 5 show that most of the compared models correctly performed the covariate selection on low dispersion data ( $\sigma = 0.2$ ), except for grLASSO, which was not able to exclude any covariate in any of the hundred replications. When evaluating the selection performance for data with greater dispersion ( $\sigma = 20$ ), we can observe in Table 6 that only the two versions of the proposed model ( $\mu$  as a hyperparameter and as a parameter) were able to identify the true two variables that were used in the construction of synthetic data (3<sup>rd</sup> and 5<sup>th</sup>) in almost all replications.

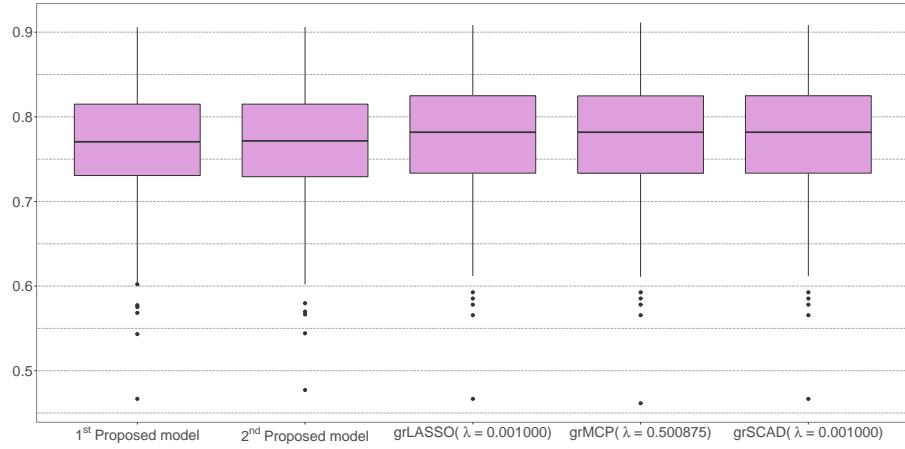
It is worth noticing that the  $\lambda = \sqrt{2}$  used in the versions of the proposed model was the lowest possible value for it since uniqueness problems in the stationary distribution begin to appear for smaller values of this parameter as a result of the combination of two factors: low regularization and multicollinearity of the covariate matrix. Therefore, this was a configuration with the lowest possible regularization, and the proposed model versions under this scenario were able to provide a good fit to the data while being able to select the variables correctly. In contrast, as noted earlier, the grLASSO, grSCAD and grMCP models face difficulties reconciling accuracy in the selection and quality of fit.

Figure 8 and Supplementary Figure 7 present the results regarding the performance metric in (7) and MSE, respectively, for the best model configurations. The metric (7) was used as a reference for choosing the best model configurations to be compared in Figure 8, as it was done for Tables 5 and 6. At the same time, for Supplementary Figure 7, the MSE itself was the reference metric for defining the best model settings. Thus, the comparison via MSE becomes fair. Turning the analysis to the results from data with low dispersion ( $\sigma = 0.2$ ), regardless of the metric being analyzed, slightly better performance of the competing methods can be observed in comparison to the two versions of the proposed model, especially when using the metric (7) as a reference. As for the data with greater dispersion, the models present similar goodness of fit and estimation accuracy.

Finally, Figure 9 shows the estimates obtained in each replication for the third and fifth functional coefficients for each model and each level of data dispersion. In this case, the performance metric in (7) was used as a reference for choosing the model configurations to be compared. When  $\sigma = 20$ , it is noticeable that there is a smaller dispersion of the estimated functional coefficients in the versions of the proposed model compared to the competing models. This observation is valid both for the third and fifth functional coefficients.



(a) Data with  $\sigma = 0.2$ .



(b) Data with  $\sigma = 20$ .

Figure 8: Boxplots of the metric (7), according to the model used and the data dispersion degree. The “1<sup>st</sup> Proposed Model” is considered to be the version with  $\lambda = \sqrt{2}$  and  $\mu$  as a parameter, while the “2<sup>nd</sup> Proposed Model” is the version with  $\lambda = \sqrt{2}$  and  $\mu$  as a hyperparameter ( $\mu = 0.3$  for  $\sigma = 0.2$  and  $\mu = 0.5$  for  $\sigma = 20$ ).

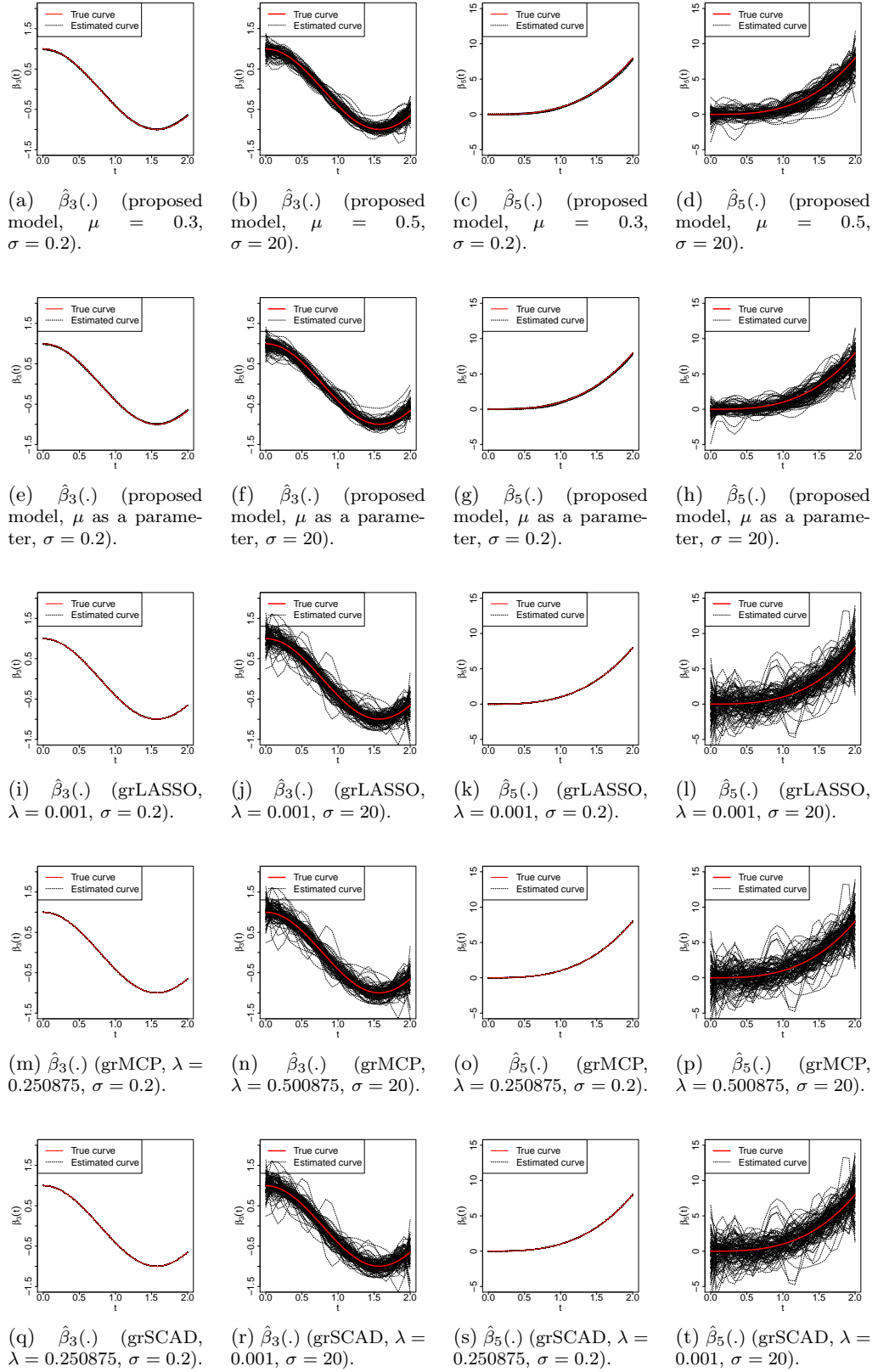


Figure 9: Partial functional coefficients (3<sup>rd</sup> and 5<sup>th</sup>, true in red and estimated for the replications in which the coefficients were selected in black), according to the data dispersion degree and model used.

### 3.5 BGLSS versus proposed model

To complete the comparisons with other existing methods, here is a brief comparative analysis between the proposed model and the Bayesian Group LASSO with Spike and Slab prior (BGLSS) method. The BGLSS method (Kyung et al., 2010) deals with the Bayesian regularization and estimation problem, taking into account the existence of groups of variables. In this case, the variables of the same group must be selected or excluded together. The BGLSS function from the R package *MBSGS* was used to implement BGLSS. In this case, the *default* function was used (also with 10000 MCMC iterations, with 5000 for burn-in). Finally, the groups of scalar coefficients ( $b_{i,l}$ 's) were defined in the same way as was done in the previous section for the other methods (grLASSO, grSCAD and grMCP), meaning the respective scalar coefficients from this expansion end up forming a group for each expansion based on a given  $\beta_l(\cdot)$ .

As the BGLSS function returns the entire chain, estimates can be calculated separately using the `map_estimate` function. Thus, we have a summary measure in accordance with the one used in the other methods (*Maximum a Posteriori* - MAP). The chains obtained in certain replications for certain coefficients can be sparse, and this can make using the `map_estimate` function unfeasible, but this is not a problem in this case since there are many values numerically equal to zero and, therefore, the MAP estimate is zero itself. A relevant fact to be highlighted is that the simulated data used in this study are the same used in the previous comparative study.

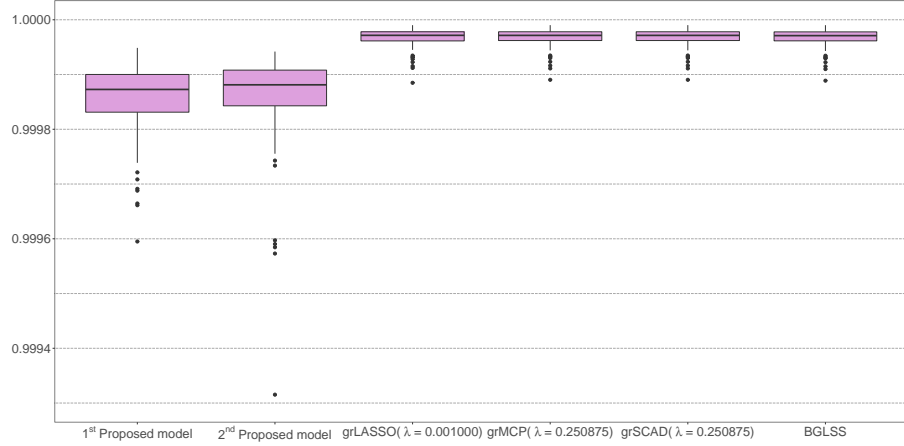
Figure 10 and Supplementary Figure 8 show the boxplots for each of the performance metrics (metric (7) and MSE, respectively). In one replication with low dispersion, the BGLSS method had its worst performance resulting in an outlier in the BGLSS boxplots (for both evaluated metrics and only for  $\sigma = 0.2$ ). Figure 10 and Supplementary Figure 8 omit this outlier since we adjusted the scale to focus on the interquartile range region to enable the comparison between the boxplots. In terms of the goodness-of-fit metric (7), as shown in Figure 10, the BGLSS method can remain competitive. It is worth highlighting that the methods present a reasonably equivalent performance in this regard and that although the competing methods perform better than the two versions of the model proposed in the scenario with the low dispersion data ( $\sigma = 0.2$ ), this difference is negligible ( $< 0.02\%$ ).

Table 7 demonstrates the variable selection capacity of the BGLSS method, presenting the proportions calculated as the number of times that each functional coefficient estimate was different from zero among the 100 replications. Unlike the grLASSO, grSCAD and grMCP methods, the BGLSS method can select the variables well even in the study with more data dispersion. It is the only one among the studied models that can compete with our proposed methodology in terms of predictive quality (through the metric (7) and MSE) and variable selection capacity.

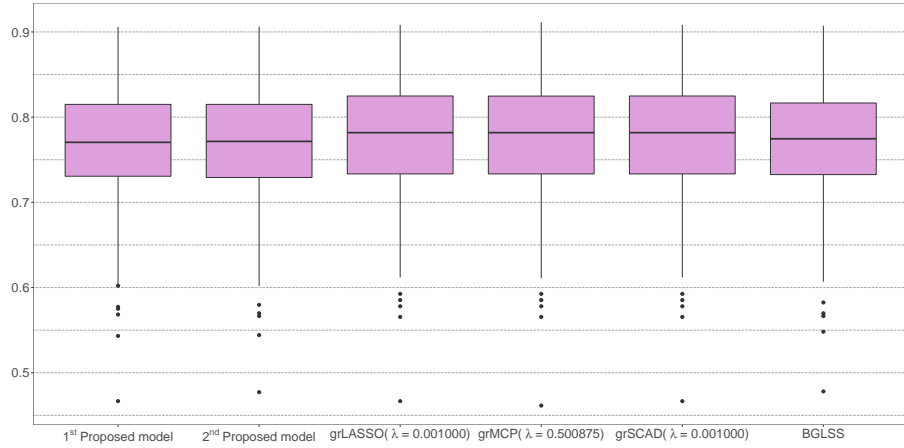
Concluding the comparative study, Figure 11 presents the estimates from the BGLSS method for the third and fifth functional coefficients. We can also observe that the BGLSS method leads to a smaller dispersion of the estimated functional coefficient curves when compared to the grLASSO, grSCAD and grMCP methods (see Figure 9). At the same time, it yields a dispersion that matches the levels of dispersion in the generated data.

## 4 Application to real data and the GCV criterion

We considered two databases to evaluate the performance of the proposed model on a set of real data: the first with COVID-19 data freely available through the Brasil.IO accessible



(a) Data with  $\sigma = 0.2$ .



(b) Data with  $\sigma = 20$ .

Figure 10: Boxplots of the metric (7), according to the model used and the data dispersion degree. The “1<sup>st</sup> Proposed Model” is considered to be the version with  $\lambda = \sqrt{2}$  and  $\mu$  as a parameter, while the “2<sup>nd</sup> Proposed Model” is the version with  $\lambda = \sqrt{2}$  and  $\mu$  as a hyperparameter ( $\mu = 0.3$  for  $\sigma = 0.2$  and  $\mu = 0.5$  for  $\sigma = 20$ ).

open data portal (Álvaro Justen et al., 2021) for the definition of the response variable of the study; and the second with the socioeconomic data of the states and the Federal District made available by the IBGE (Brazilian Institute of Geography and Statistics) for the definition of the covariates for our analysis.

The response variable chosen for this study is the logarithm of the accumulated weekly number of deaths per 10 000 inhabitants due to COVID-19 in the Brazilian states and the Federal District. Therefore, there are  $m = 27$  curves corresponding to the 26 states plus the Federal District. As the first cases of COVID-19 in each state appeared at different weeks, we decided to analyze the data from the 20th epidemiological week of 2020, the week from which new cases were already registered in all of the federation members (the 26 states and the Federal District), until the 32nd epidemiological week of the year 2021, totalling 66 weeks ( $n_i = n = 66$ ).

Next, nine covariates were defined ( $p = 9$ ) as explanatory variables, which are:



Table 7: Proportion of non-zero estimates for each functional coefficient from the BGLSS method among the 100 replications, according to the data dispersion degree.

$\hat{\beta}_l(\cdot)$	$\sigma$	
	0.2	20
$\hat{\beta}_1(\cdot)$	0	0.03
$\hat{\beta}_2(\cdot)$	0.01	0.01
$\hat{\beta}_3(\cdot)$	1	1
$\hat{\beta}_4(\cdot)$	0	0.01
$\hat{\beta}_5(\cdot)$	0.99	0.99
$\hat{\beta}_6(\cdot)$	0.01	0.02

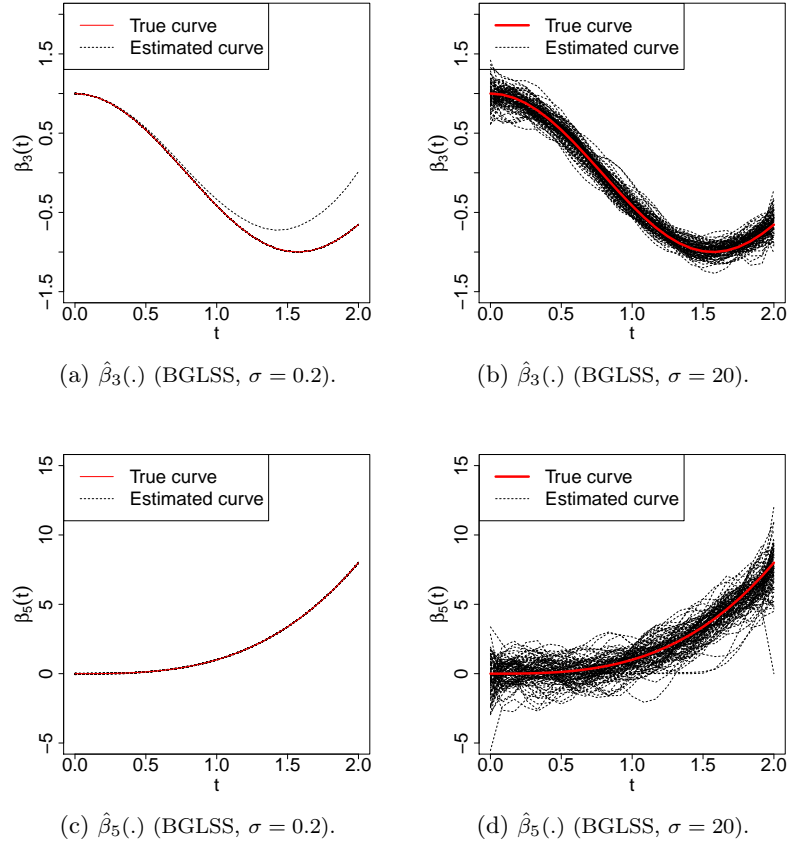


Figure 11: Partial functional coefficients ( $3^{\text{rd}}$  and  $5^{\text{th}}$ , true in red and estimated for the replications in which the coefficients were selected in black) from the BGLSS method, according to the data dispersion degree.

- demographic density;
- HDI (Human Development Index);
- Gini index of the per capita household income distribution;
- unemployment rate of people aged 14 or over;
- QoLLI (Quality of Life Loss Index);
- percentage of population with health insurance;
- number of hospital beds per 10 000 inhabitants;
- number of doctors per 10 000 inhabitants;
- average real income from the main job usually earned per month by persons aged 14 years or over (income).

The design matrix was defined with the covariates positioned in the same order in which they were presented above, so we have  $Z_1\beta_1(\cdot)$  as the functional coefficient associated with the demographic density,  $Z_2\beta_2(\cdot)$  as a functional coefficient associated with the HDI, and so on. In addition, the covariates were standardized by their mean and standard deviation before applying the model (see Section 1 of the Supplementary Material). In addition, the intercept was estimated as described in Section 3.1.

The Gibbs sampler implemented the proposed Bayesian model using two chains to enable a convergence diagnosis. The initialization of the chains, the maximum number of iterations, the choice of the *burn-in* period, the spacing of points between sampled values, as well as the choice of the hyperparameters and obtaining the Bayesian estimates were all established following what was described in Section 3.1 for the studies with synthetic data. Furthermore, we considered the model with  $\mu$  as a parameter in this study.

Before presenting any results, it is worth mentioning that B-splines were used for the basis expansion of all partial functional coefficients, considering three values for  $K$  ( $K = 5$ ,  $K = 10$  and  $K = 15$ ). The diagnostic analysis based on the method proposed by Gelman and Rubin (1992) attested for the convergence of the chains of the partial coefficients in all tested model configurations after the period of *burn-in*.

Unfortunately, it is impossible to calculate the MSE between the points of the estimated curve and those of the true curve in a study with real data since the true curve is unknown. Since calculating the MSE from the distances between the observed values and the points on the estimated curve is not recommended due to the possibility of *overfitting*, we consider an alternative measure based on a cross-validation procedure. Although the conventional cross-validation associated with the MSE is an effective procedure to overcome the problem of *overfitting*, it often becomes inefficient due to the high computational cost. As an alternative to the cross-validation procedure, there is the Generalized Cross Validation (GCV) (Golub et al., 1979). Adapting the GCV criterion presented by Golub et al. (1979) to the reality of the proposed model, we obtain

$$\begin{aligned} \text{GCV}(K) &= \frac{1}{\sum_{i=1}^m n_i} \frac{\sum_{i=1}^m \sum_{j=1}^{n_i} (\tilde{y}_{ij} - \sum_{l=1}^p x_{li} \hat{Z}_l \hat{\beta}_l(t_{ij}))' (\tilde{y}_{ij} - \sum_{l=1}^p x_{li} \hat{Z}_l \hat{\beta}_l(t_{ij}))}{\left[1 - \frac{1}{\sum_{i=1}^m n_i} \text{tr}(\mathbf{S}_K)\right]^2} \\ &= \frac{1}{\sum_{i=1}^m n_i} \frac{(\tilde{\mathbf{y}}_{..} - \hat{\mathbf{O}}_{..} \hat{\mathbf{b}})' (\tilde{\mathbf{y}}_{..} - \hat{\mathbf{O}}_{..} \hat{\mathbf{b}})}{\left[1 - \frac{1}{\sum_{i=1}^m n_i} \text{tr}(\mathbf{S}_K)\right]^2}, \end{aligned}$$

Table 8: Values of the metric (7) and the GCV criterion, according to the value of  $K$  used in the model.

Metric	$K$		
	5	10	15
Metric (7)	0.44907	0.11603	0.14010
GCV	0.59545	0.94175	0.91838

where  $\tilde{y}_{ij} = y_{ij} - \tilde{\beta}_0(t_{ij})$ ,  $\mathbf{S}_K$  is the projection matrix of the proposed model with  $K$  bases on the expansions of the functional coefficients,  $\hat{\mathbf{O}}_{\dots}$  is the estimate for  $\mathbf{O}_{\dots}$  (as defined in Appendix A) and  $\hat{\mathbf{b}}$  is the estimate for  $\mathbf{b}$ .

To understand how  $\mathbf{S}_K$  is calculated, note that the mean of the complete conditional distribution of  $\mathbf{b}$ , which is equivalent to the mode since the normal distribution is symmetric, is given as follows:

$$E(\mathbf{b}|\boldsymbol{\theta}, \boldsymbol{\mu}, \sigma^2, \boldsymbol{\tau}^2, \mathbf{Z}, \mathbf{y}) = \mathbf{Q}^{-1} \mathbf{O}_{\dots}' \tilde{\mathbf{y}}_{\dots},$$

as shown in the details of the full conditional distribution for  $\mathbf{b}$  in Appendix A. Finally, when considering  $\hat{\mathbf{b}} = \hat{\mathbf{Q}}^{-1} \hat{\mathbf{O}}_{\dots}' \tilde{\mathbf{y}}_{\dots}$ , in which  $\hat{\mathbf{Q}}$  and  $\hat{\mathbf{O}}_{\dots}$  are the respective estimates of  $\mathbf{Q}$  (also defined in Appendix A) and  $\mathbf{O}_{\dots}$ , then the estimated curve is represented by

$$\hat{\mathbf{y}}_{\dots} = \hat{\mathbf{O}}_{\dots} \hat{\mathbf{b}} = \hat{\mathbf{O}}_{\dots} \hat{\mathbf{Q}}^{-1} \hat{\mathbf{O}}_{\dots}' \tilde{\mathbf{y}}_{\dots},$$

so that the projection matrix can be represented by

$$\mathbf{S}_K = \hat{\mathbf{O}}_{\dots} \hat{\mathbf{Q}}^{-1} \hat{\mathbf{O}}_{\dots}'.$$

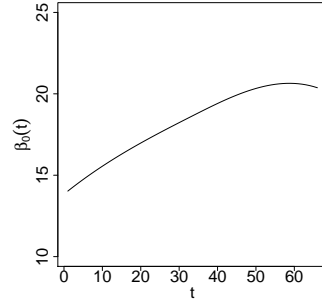
Therefore, it becomes completely possible to calculate the GCV(.) for all models tested as we vary  $K$ . The smaller the GCV value, the better the fit.

Table 8 presents the value of the metric in (7) and the GCV criterion for each  $K$  number of basis functions considered. We can observe that the fit quality is better with  $K = 5$ , regardless of the metric used for analysis. Because the functional response data are observational, it is natural that the metric in (7) is not so close to one as they were in the simulation studies. Still, even with a reasonably low number of curves ( $m = 27$ ), the model with  $K = 5$  can return a value of almost 45% for that metric.

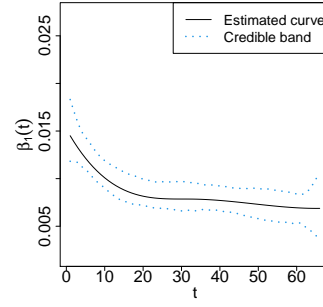
Figure 12 presents the estimated curves and the credible bands for the functional coefficients ( $\hat{Z}_l \hat{\beta}_l(\cdot)$ ) associated with the covariates that were selected by the proposed model with  $K = 5$ . At the same time, Supplementary Figure 9 shows the estimated curves of the partial functional coefficients ( $\hat{\beta}_l(\cdot)$ ) associated with the covariates that were excluded. It is worth remembering that the estimated value for the functional coefficients associated with the covariates that were excluded is equal to zero for every  $t$  point. Therefore, Supplementary Figure 9 presents only the estimated curves of the partial functional coefficients.

Observing the posterior samples of each  $Z_l$  (not shown here), we notice that there was perfect agreement between the points of the posterior samples and the summary statistics since the respective samples for  $\hat{Z}_l$ 's equal to zero are entirely characterized by zeros. Similarly, the respective samples for  $\hat{Z}_l$ 's equal to one are entirely characterized by ones. This reinforces the little uncertainty that the model has to define which variables should remain and which ones should be excluded from the model.

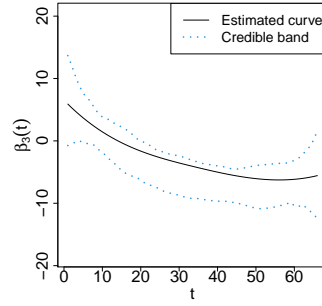
The Gini index and QoLLI covariates were the most influential for predicting the response variable since their respective functional coefficients are found on a larger scale. It



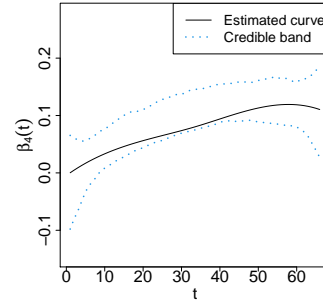
(a) Estimated  $\beta_0(t)$  (Intercept).



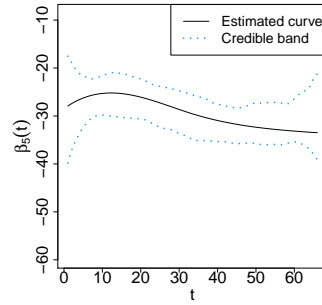
(b) Estimated  $\beta_1(t)$  (Demographic density).



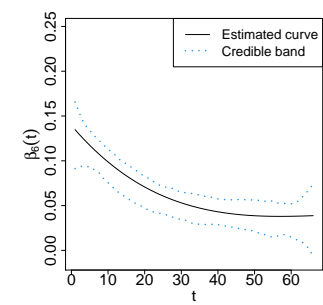
(c) Estimated  $\beta_3(t)$  (Gini index).



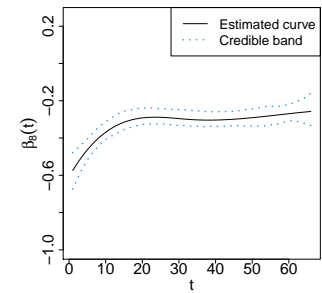
(d) Estimated  $\beta_4(t)$  (unemployment rate).



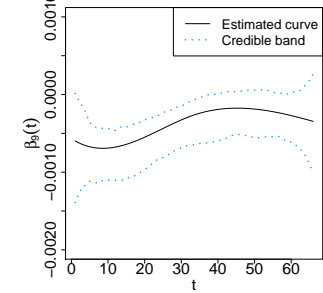
(e) Estimated  $\beta_5(t)$  (QoLLI).



(f) Estimated  $\beta_6(t)$  (Percentage of population with health insurance).



(g) Estimated  $\beta_8(t)$  (Number of doctors per 10000 inhabitants).



(h) Estimated  $\beta_9(t)$  (Income).

Figure 12: Estimated curves for the functional coefficients associated with the covariates that were selected by the proposed model with  $K = 5$  basis functions.

is worth remembering that any analysis of the results must take into account that they are conditioned to some initial determining factors, such as the initial set of candidate covariates in the model and the hypothesis of linearity.

## 5 Final considerations

This work focuses on functional data modeling and proposes a model-based approach under the Bayesian paradigm for variable selection in FOSR. The proposed methodology shows low sensitivity to the hyperparameter  $\mu$ , which is desirable since this component does not control the regularization. On the other hand,  $\lambda$  plays the role of a regularization hyperparameter, and naturally, the model has some sensitivity to it. If desired, it is still possible to add a Gamma prior to  $\lambda^2$ , leading to an improper prior and guaranteeing minor sensitivity of the model to  $\lambda$ . However, in this case,  $\lambda$  would no longer play the role of regularizer and uniqueness problems in the stationary distribution could appear if there is multicollinearity between the covariates.

Through simulations, the proposed model proved superior in correctly selecting the covariates compared with other variable selection methods in FOSR. At the same time, it maintained an optimal level of goodness of fit. The competing methods in the simulation scenario with the highest data dispersion ( $\sigma = 20$ ) could not balance selection accuracy well with the goodness of fit. Therefore, they need to lose goodness of fit and increase regularization to ensure better accuracy in the selection.

When applying the proposed variable selection model to real data, our proposed methodology could perform the variable selection. However, the fit could not explain much of the data variation (value of metric (7),  $K = 5$ , 44.9%). The not-so-great fit to the data is explained mainly by the small number of curves ( $m = 27$ ) used. As the proposed model is consistent, if the same study were carried out at the municipal level (Brazil has about 5568 municipalities, plus the Federal District and the State District of Fernando de Noronha), higher values would certainly be observed for the metric in (7), and naturally smaller values for the GCV criterion. The choice to carry out the study with state data is justified by the high computational cost generated when having  $m = 5570$ . Therefore, this limitation motivates some future work where the proposed Bayesian hierarchical model is implemented via *variational inference*.

In addition to optimizing and reducing the computational cost by approximating the posterior distribution via *variational inference*, another possibility for future work is to develop an alternative approach to verify whether the functional coefficients are only null at specific points or regions of  $t$  since the model for selecting variables proposed in this article is only able to indicate whether a covariate should be part of the model or not.

## Acknowledgments

This study was financed in part by the Coordenação de Aperfeiçoamento de Pessoal de Nível Superior – Brasil (CAPES) – Finance Code 001, by the Natural Sciences and Engineering Research Council of Canada (NSERC), grant number RGPIN-2019-05915, and FAPESP grants 2018/04654-9 and 2019/00787-7.

## References

- Aneiros, G., Ferraty, F., and Vieu, P. (2011), “Recent Advances in Functional Data Analysis and Related Topics,” *Contributions to Statistics*.
- Barber, R. F., Reimherr, M., and Schill, T. (2017), “The function-on-scalar LASSO with applications to longitudinal GWAS,” *Electronic Journal of Statistics*, 11, 1351–1389.
- Breheny, P. and Huang, J. (2013), “Group descent algorithms for nonconvex penalized linear and logistic regression models with grouped predictors,” *Statistics and Computing*, 25, 173–187.
- Breheny, P., Zeng, Y., and Kurth, R. (2021), *Regularization Paths for Regression Models with Grouped Covariates*, CRAN, r package version 3.4.0.
- CAI, X., XUE, L., CAO, J., and Initiative, A. D. N. (2022), “Robust estimation and variable selection for function-on-scalar regression,” *The Canadian Journal of Statistics*, 50, 162–179.
- Chen, Y., Goldsmith, J., and Ogden, R. T. (2016), “Variable selection in function-on-scalar regression,” *Stat*, 5, 88–101.
- Collazos, J. A., Dias, R., and Zambom, A. Z. (2016), “Consistent variable selection for functional regression models,” *Journal of Multivariate Analysis*, 146, 63–71.
- de Oliveira Sousa, P. H. T., de Souza, C. P. E., and Dias, R. (2023), “Bayesian adaptive selection of basis functions for functional data representation,” *Journal of Applied Statistics*, 1–35.
- Fan, J. and Li, R. (2001), “Variable selection via nonconcave penalized likelihood and its oracle properties,” *Journal of the American Statistical Association*, 96, 1348–1360.
- (2004), “New Estimation and Model Selection Procedures for Semiparametric Modeling in Longitudinal Data Analysis,” *Journal of the American Statistical Association*, 99, 710–723.
- Fan, Z. and Reimherr, M. (2017), “High-dimensional adaptive function-on-scalar regression,” *Econometrics and Statistics*, 1, 167–183.
- Gelman, A. and Rubin, D. B. (1992), “Inference from Iterative Simulation Using Multiple Sequences,” *Statistical Science*, 7, 457–511.
- Gertheiss, J., Maity, A., and Staicu, A.-M. (2013), “Variable selection in generalized functional linear models,” *Stat*, 2, 86–101.
- Golub, G. H., Heath, M., and Wahba, G. (1979), “Generalized Cross-Validation as a Method for Choosing a Good Ridge Parameter,” *Technometrics*, 21(2), 215–223.
- Hong, Z. and Lian, H. (2011), “Inference of Genetic Networks from Time Course Expression Data Using Functional Regression with Lasso Penalty,” *Communications in Statistics - Theory and Methods*, 40, 1768–1779.
- Horváth, L. and Kokoszka, P. (2012), *Inference for Functional Data with Applications*, Springer Science and Business Media.

- Huang, J., Breheny, P., and Ma, S. (2012), “A Selective Review of Group Selection in High-Dimensional Models,” *Statistical Science*, 27, 481–499.
- Kowal, D. R. (2018), “Dynamic Function-on-Scalars Regression,” .
- Kowal, D. R. and Bourgeois, D. C. (2020), “Bayesian Function-on-Scalars Regression for High-Dimensional Data,” *Journal of Computational and Graphical Statistics*, 29, 1–10.
- Kutner, M. H., Nachtsheim, C. J., Neter, J., and Li, W. (2004), *Applied Linear Statistical Models*, McGraw-Hill Companies, Incorporated.
- Kyung, M., Gill, J., Ghosh, M., and Casella, G. (2010), “Penalized Regression, Standard Errors, and Bayesian Lassos,” *Bayesian Analysis*, 5, 369–412.
- Ma, S., Song, Q., and Wang, L. (2013), “Simultaneous variable selection and estimation in semiparametric modeling of longitudinal/clustered data,” *Bernoulli*, 19, 252–274.
- Matsui, H. and Konishi, S. (2011), “Variable selection for functional regression models via the L1 regularization,” *Computational Statistics & Data Analysis*, 55, 3304–3310.
- Meyer, M. J., Coull, B. A., Versace, F., Cinciripini, P., and Morris, J. S. (2015), “Bayesian Function-on-Function Regression for Multilevel Functional Data,” *Biometrics*, 71, 563–574.
- Mingotti, N., Lillo, R. E., and Romo, J. (2013), “Lasso variable selection in functional regression,” *Statistics and Econometrics Series 13*, Working paper 13-14.
- Montagna, S., Tokdar, S. T., Neelon, B., and Dunson, D. B. (2012), “Bayesian Latent Factor Regression for Functional and Longitudinal Data,” *Biometrics*, 68, 1064–1073.
- Parodi, A. and Reimherr, M. (2018), “Simultaneous variable selection and smoothing for high-dimensional function-on-scalar regression,” *Electronic Journal of Statistics*, 12, 4602–4639.
- Qi, X. and Luo, R. (2018), “Function-on-function regression with thousands of predictive curves,” *Journal of Multivariate Analysis*, 163, 51–66.
- Ramsay, J. and Silverman, B. (2005), *Functional Data Analysis*, Springer Series in Statistics.
- Reiss, P. T., Goldsmith, J., Shang, H. L., and Ogden, R. T. (2017), “Methods for Scalar-on-Function Regression,” *International Statistical Review*, 85(2), 228–249.
- Rencher, A. and Schaalje, G. (2008), *Linear Models in Statistics*, Wiley.
- Tibshirani, R. (1996), “Regression Shrinkage and Selection via the Lasso,” *Journal of the Royal Statistical Society*, 58, 267–288.
- Wang, L., Chen, G., and Li, H. (2007), “Group SCAD regression analysis for microarray time course gene expression data,” *Bioinformatics*, 23, 1486–1494.
- Weisberg, S. (2013), *Applied Linear Regression*, Wiley Series in Probability and Statistics, Wiley.

- Yuan, M. and Lin, Y. (2006), “Model Selection and Estimation in Regression with Grouped Variables,” *Journal of the Royal Statistical Society, Series B (Statistical Methodology)*, 68(1), 49–67.
- Zhang, C.-H. (2010), “Nearly unbiased variable selection under minimax concave penalty,” *The Annals of Statistics*, 38, 894–942.
- Álvaro Justen et al. (2021), “COVID-19: Boletins informativos e casos do coronavírus,” [https://brasil.io/dataset/covid19/caso\\_full/](https://brasil.io/dataset/covid19/caso_full/), [Online; accessed 17-August-2021; Licença: Creative Commons Attribution-ShareAlike 4.0 International (CC BY-SA 4.0)].



## A Full conditional distributions

First, consider  $g_i(t_{ij}) = \sum_{l=1}^p \sum_{k=1}^K x_{li} Z_l b_{kl} B_k(t_{ij})$ , so that

$$y_{ij} = \beta_0(t_{ij}) + g_i(t_{ij}) + \epsilon_{ij} = \sum_{k=1}^K b_{k0} B_k(t_{ij}) + g_i(t_{ij}) + \epsilon_{ij}.$$

We obtain the full conditional distributions of the coefficients  $\mathbf{b}$ 's as follows:

$$\begin{aligned} & f(\mathbf{b}|\boldsymbol{\theta}, \boldsymbol{\mu}, \sigma^2, \boldsymbol{\tau}^2, \mathbf{Z}, \mathbf{y}) \\ & \propto \pi(\sigma^2) \pi(\boldsymbol{\tau}^2) \pi(\boldsymbol{\mu}) f(\boldsymbol{\theta}|\boldsymbol{\mu}) f(\mathbf{b}|\sigma^2, \boldsymbol{\tau}^2) p(\mathbf{Z}|\boldsymbol{\theta}) f(\mathbf{y}|\mathbf{b}, \mathbf{Z}, \sigma^2) \\ & \propto f(\mathbf{b}|\sigma^2, \boldsymbol{\tau}^2) f(\mathbf{y}|\mathbf{b}, \mathbf{Z}, \sigma^2) \\ & \propto \left[ \prod_{k=1}^K \prod_{l=1}^p f(b_{kl}|\sigma^2, \tau_{kl}^2) \right] \left[ \prod_{i=1}^m \prod_{j=1}^{n_i} f(y_{ij}|\mathbf{b}, \mathbf{Z}, \sigma^2) \right] \\ & \propto \exp \left\{ - \sum_{k=1}^K \sum_{l=1}^p \frac{b_{kl}^2}{2\sigma^2 \tau_{kl}^2} \right\} \exp \left\{ - \frac{\sum_{i=1}^m \sum_{j=1}^{n_i} (y_{ij} - \beta_0(t_{ij}) - g_i(t_{ij}))^2}{2\sigma^2} \right\} \\ & \propto \exp \left\{ - \frac{\sum_{k=1}^K \sum_{l=1}^p \frac{b_{kl}^2}{\tau_{kl}^2}}{2\sigma^2} \right\} \exp \left\{ - \frac{\sum_{i=1}^m \sum_{j=1}^{n_i} (\tilde{y}_{ij} - g_i(t_{ij}))^2}{2\sigma^2} \right\}, \end{aligned}$$

in which  $\tilde{y}_{ij} = y_{ij} - \beta_0(t_{ij})$ .

Remembering that  $g_i(t_{ij}) = \sum_{l=1}^p \sum_{k=1}^K x_{li} Z_l b_{kl} B_k(t_{ij})$ , considering

$$\mathbf{O}_{lij} = (x_{li} Z_l B_1(t_{ij}), x_{li} Z_l B_2(t_{ij}), \dots, x_{li} Z_l B_K(t_{ij}))',$$

a dimension vector  $(K \times 1)$ , and calculating

$$\mathbf{O}_{.ij} = \begin{pmatrix} \mathbf{O}_{1ij} \\ \mathbf{O}_{2ij} \\ \vdots \\ \mathbf{O}_{pij} \end{pmatrix}_{(Kp \times 1)},$$

so we have  $g_i(t_{ij}) = \mathbf{b}' \mathbf{O}_{.ij}$ .

As such,  $\boldsymbol{\eta}^2 = (\boldsymbol{\eta}_{.1}^2, \boldsymbol{\eta}_{.2}^2, \dots, \boldsymbol{\eta}_{.p}^2)'$ , in which  $\boldsymbol{\eta}_{.l}^2 = (\frac{1}{\tau_{1l}^2}, \frac{1}{\tau_{2l}^2}, \dots, \frac{1}{\tau_{Kl}^2})'$ , so we have

$$\begin{aligned} & f(\mathbf{b}|\boldsymbol{\theta}, \boldsymbol{\mu}, \sigma^2, \boldsymbol{\tau}^2, \mathbf{Z}, \mathbf{y}) \\ & \propto \exp \left\{ - \frac{\mathbf{b}' \text{diag}(\boldsymbol{\eta}^2) \mathbf{b} + \sum_{i=1}^m \sum_{j=1}^{n_i} (\tilde{y}_{ij} - \mathbf{b}' \mathbf{O}_{.ij})' (\tilde{y}_{ij} - \mathbf{b}' \mathbf{O}_{.ij})}{2\sigma^2} \right\} \\ & \propto \exp \left\{ - \frac{\mathbf{b}' \text{diag}(\boldsymbol{\eta}^2) \mathbf{b} + \sum_{i=1}^m \sum_{j=1}^{n_i} [\tilde{y}_{ij}^2 - 2\tilde{y}_{ij} \mathbf{b}' \mathbf{O}_{.ij} + \mathbf{b}' \mathbf{O}_{.ij} \mathbf{O}_{.ij}' \mathbf{b}]}{2\sigma^2} \right\} \\ & \propto \exp \left\{ - \frac{\mathbf{b}' [\text{diag}(\boldsymbol{\eta}^2) + \sum_{i=1}^m \sum_{j=1}^{n_i} \mathbf{O}_{.ij} \mathbf{O}_{.ij}'] \mathbf{b} - 2\mathbf{b}' \sum_{i=1}^m \sum_{j=1}^{n_i} \mathbf{O}_{.ij} \tilde{y}_{ij}}{2\sigma^2} \right\}. \end{aligned}$$

By the Cholesky decomposition, let  $\mathbf{Q} = \left[ \text{diag}(\boldsymbol{\eta}^2) + \sum_{i=1}^m \sum_{j=1}^{n_i} \mathbf{O}_{.ij} \mathbf{O}_{.ij}' \right] = \mathbf{L}_i \mathbf{L}_i'$ , a matrix of dimension  $(Kp \times Kp)$ , then

$$\begin{aligned}
& f(\mathbf{b}|\boldsymbol{\theta}, \boldsymbol{\mu}, \sigma^2, \boldsymbol{\tau}^2, \mathbf{Z}, \mathbf{y}) \\
& \propto \exp \left\{ -\frac{\mathbf{b}' \mathbf{L}_i \mathbf{L}_i' \mathbf{b} - 2\mathbf{b}' \sum_{i=1}^m \sum_{j=1}^{n_i} \mathbf{O}_{.ij} \tilde{\mathbf{y}}_{ij}}{2\sigma^2} \right\} \\
& \propto \exp \left\{ -\frac{(\mathbf{L}_i' \mathbf{b})' \mathbf{L}_i' \mathbf{b} - 2\mathbf{b}' \mathbf{L}_i \mathbf{L}_i^{-1} \sum_{i=1}^m \sum_{j=1}^{n_i} \mathbf{O}_{.ij} \tilde{\mathbf{y}}_{ij}}{2\sigma^2} \right\} \\
& \propto \exp \left\{ -\frac{(\mathbf{L}_i' \mathbf{b})' \mathbf{L}_i' \mathbf{b} - 2(\mathbf{L}_i' \mathbf{b})' \mathbf{L}_i^{-1} \sum_{i=1}^m \sum_{j=1}^{n_i} \mathbf{O}_{.ij} \tilde{\mathbf{y}}_{ij}}{2\sigma^2} \right\} \\
& \propto \exp \left\{ -\frac{(\mathbf{L}_i' \mathbf{b} - \mathbf{L}_i^{-1} \sum_{i=1}^m \sum_{j=1}^{n_i} \mathbf{O}_{.ij} \tilde{\mathbf{y}}_{ij})' (\mathbf{L}_i' \mathbf{b} - \mathbf{L}_i^{-1} \sum_{i=1}^m \sum_{j=1}^{n_i} \mathbf{O}_{.ij} \tilde{\mathbf{y}}_{ij})}{2\sigma^2} \right\} \\
& \propto \exp \left\{ -\frac{(\mathbf{L}_i' \mathbf{b} - \mathbf{L}_i^{-1} \sum_{i=1}^m \sum_{j=1}^{n_i} \mathbf{O}_{.ij} \tilde{\mathbf{y}}_{ij})' \mathbf{L}_i^{-1} \mathbf{L}_i \mathbf{L}_i' (\mathbf{L}_i')^{-1} (\mathbf{L}_i' \mathbf{b} - \mathbf{L}_i^{-1} \sum_{i=1}^m \sum_{j=1}^{n_i} \mathbf{O}_{.ij} \tilde{\mathbf{y}}_{ij})}{2\sigma^2} \right\} \\
& \propto \exp \left\{ -\frac{(\mathbf{b} - (\mathbf{L}_i \mathbf{L}_i')^{-1} \sum_{i=1}^m \sum_{j=1}^{n_i} \mathbf{O}_{.ij} \tilde{\mathbf{y}}_{ij})' \mathbf{L}_i \mathbf{L}_i' (\mathbf{b} - (\mathbf{L}_i \mathbf{L}_i')^{-1} \sum_{i=1}^m \sum_{j=1}^{n_i} \mathbf{O}_{.ij} \tilde{\mathbf{y}}_{ij})}{2\sigma^2} \right\} \\
& \Rightarrow
\end{aligned}$$

$$\begin{aligned}
& f(\mathbf{b}|\boldsymbol{\theta}, \boldsymbol{\mu}, \sigma^2, \boldsymbol{\tau}^2, \mathbf{Z}, \mathbf{y}) = f(\mathbf{b}|\sigma^2, \boldsymbol{\tau}^2, \mathbf{Z}, \mathbf{y}) \\
& \propto \exp \left\{ -\frac{(\mathbf{b} - \mathbf{Q}^{-1} \sum_{i=1}^m \sum_{j=1}^{n_i} \mathbf{O}_{.ij} \tilde{\mathbf{y}}_{ij})' (\mathbf{Q}^{-1})^{-1} (\mathbf{b} - \mathbf{Q}^{-1} \sum_{i=1}^m \sum_{j=1}^{n_i} \mathbf{O}_{.ij} \tilde{\mathbf{y}}_{ij})}{2\sigma^2} \right\}. \quad (9)
\end{aligned}$$

So,  $f(\mathbf{b}|\boldsymbol{\theta}, \boldsymbol{\mu}, \sigma^2, \boldsymbol{\tau}^2, \mathbf{Z}, \mathbf{y})$  is precisely a Multivariate Normal distribution with mean  $\mathbf{Q}^{-1} \sum_{i=1}^m \sum_{j=1}^{n_i} \mathbf{O}_{.ij} \tilde{\mathbf{y}}_{ij}$  and variance  $\sigma^2 \mathbf{Q}^{-1}$ .

The mean of this Normal distribution can still be described in a simplified way. When considering

$$\mathbf{O}_{\dots} = \begin{pmatrix} \mathbf{O}_{.11}' \\ \mathbf{O}_{.12}' \\ \vdots \\ \mathbf{O}_{.1n_1}' \\ \vdots \\ \mathbf{O}_{.m1}' \\ \mathbf{O}_{.m2}' \\ \vdots \\ \mathbf{O}_{.mn_m}' \end{pmatrix}_{(\sum_{i=1}^m n_i \times Kp)} = \begin{pmatrix} \mathbf{O}_{111}' & \mathbf{O}_{211}' & \dots & \mathbf{O}_{p11}' \\ \mathbf{O}_{112}' & \mathbf{O}_{212}' & \dots & \mathbf{O}_{p12}' \\ \vdots & \vdots & \ddots & \vdots \\ \mathbf{O}_{11n_1}' & \mathbf{O}_{21n_1}' & \dots & \mathbf{O}_{p1n_1}' \\ \vdots & \vdots & \ddots & \vdots \\ \mathbf{O}_{1m1}' & \mathbf{O}_{2m1}' & \dots & \mathbf{O}_{pm1}' \\ \mathbf{O}_{1m2}' & \mathbf{O}_{2m2}' & \dots & \mathbf{O}_{pm2}' \\ \vdots & \vdots & \ddots & \vdots \\ \mathbf{O}_{1mn_m}' & \mathbf{O}_{2mn_m}' & \dots & \mathbf{O}_{pmn_m}' \end{pmatrix}_{(\sum_{i=1}^m n_i \times Kp)},$$

so we have

$$\mathbb{E}(\mathbf{b}|\boldsymbol{\theta}, \boldsymbol{\mu}, \sigma^2, \boldsymbol{\tau}^2, \mathbf{Z}, \mathbf{y}) = \mathbf{Q}^{-1} \mathbf{O}_{\dots}' \tilde{\mathbf{y}}_{\dots},$$

in which  $\tilde{\mathbf{y}}_{\dots} = (\tilde{\mathbf{y}}_{1.}', \tilde{\mathbf{y}}_{2.}', \dots, \tilde{\mathbf{y}}_{m.}')'$  and each  $\tilde{\mathbf{y}}_{i.} = (\tilde{y}_{i1}, \tilde{y}_{i2}, \dots, \tilde{y}_{in_i})'$ .

Similarly, we obtain the full conditionals of the  $\theta_l$ 's, taking

$$\begin{aligned} & f(\theta_l | \mathbf{b}, \boldsymbol{\theta}_{-[l]}, \boldsymbol{\mu}, \sigma^2, \boldsymbol{\tau}^2, \mathbf{Z}, \mathbf{y}) \\ & \propto \pi(\sigma^2) \pi(\boldsymbol{\tau}^2) \pi(\boldsymbol{\mu}) f(\theta_l | \mu_l) f(\boldsymbol{\theta}_{-[l]} | \boldsymbol{\mu}_{-[l]}) f(\mathbf{b} | \sigma^2, \boldsymbol{\tau}^2) p(\mathbf{Z} | \boldsymbol{\theta}) p(\mathbf{y} | \mathbf{b}, \mathbf{Z}, \sigma^2) \\ & \propto f(\theta_l | \mu_l) p(Z_l | \theta_l) \propto (\theta_l)^{\mu_l - 1} (1 - \theta_l)^{(1 - \mu_l) - 1} (\theta_l)^{Z_l} (1 - \theta_l)^{1 - Z_l} \end{aligned}$$

$\Rightarrow$

$$\begin{aligned} f(\theta_l | \mathbf{b}, \boldsymbol{\theta}_{-[l]}, \boldsymbol{\mu}, \sigma^2, \boldsymbol{\tau}^2, \mathbf{Z}, \mathbf{y}) &= f(\theta_l | \mu_l, Z_l) \\ &\propto (\theta_l)^{\mu_l + Z_l - 1} (1 - \theta_l)^{(1 - \mu_l) - Z_l + 1 - 1}. \end{aligned} \quad (10)$$

Which shows that  $f(\theta_l | \mathbf{b}, \boldsymbol{\theta}_{-[l]}, \boldsymbol{\mu}, \sigma^2, \boldsymbol{\tau}^2, \mathbf{Z}, \mathbf{y})$  is a beta with the first parameter being  $\mu_l + Z_l$  and the second being  $2 - Z_l - \mu_l$ .

In order to obtain the full conditional distributions of the latent variables, it is necessary to calculate the probability

$$\begin{aligned} & P(Z_l = 1 | \mathbf{b}, \boldsymbol{\theta}, \boldsymbol{\mu}, \sigma^2, \boldsymbol{\tau}^2, \mathbf{Z}_{-[l]}, \mathbf{y}) \\ &= \frac{\pi(\sigma^2) \pi(\boldsymbol{\tau}^2) \pi(\boldsymbol{\mu}) f(\boldsymbol{\theta} | \boldsymbol{\mu}) f(\mathbf{b} | \sigma^2, \boldsymbol{\tau}^2) P(Z_l = 1 | \boldsymbol{\theta}) P(\mathbf{Z}_{-[l]} = \mathbf{z}_{-[l]} | \boldsymbol{\theta}) f(\mathbf{y} | \mathbf{b}, Z_l = 1, \mathbf{Z}_{-[l]} = \mathbf{z}_{-[l]}, \sigma^2)}{\sum_{z=0}^1 \pi(\sigma^2) \pi(\boldsymbol{\tau}^2) \pi(\boldsymbol{\mu}) f(\boldsymbol{\theta} | \boldsymbol{\mu}) f(\mathbf{b} | \sigma^2, \boldsymbol{\tau}^2) P(Z_l = z | \boldsymbol{\theta}) P(\mathbf{Z}_{-[l]} = \mathbf{z}_{-[l]} | \boldsymbol{\theta}) f(\mathbf{y} | \mathbf{b}, Z_l = z, \mathbf{Z}_{-[l]} = \mathbf{z}_{-[l]}, \sigma^2)} \\ &= \frac{P(Z_l = 1 | \boldsymbol{\theta}) P(\mathbf{Z}_{-[l]} = \mathbf{z}_{-[l]} | \boldsymbol{\theta}) f(\mathbf{y} | \mathbf{b}, Z_l = 1, \mathbf{Z}_{-[l]} = \mathbf{z}_{-[l]}, \sigma^2)}{\sum_{z=0}^1 P(Z_l = z | \boldsymbol{\theta}) P(\mathbf{Z}_{-[l]} = \mathbf{z}_{-[l]} | \boldsymbol{\theta}) f(\mathbf{y} | \mathbf{b}, Z_l = z, \mathbf{Z}_{-[l]} = \mathbf{z}_{-[l]}, \sigma^2)}. \end{aligned}$$

Simplifying this, we have

$$\begin{aligned} &= \frac{\theta_l f(\mathbf{y} | \mathbf{b}, Z_l = 1, \mathbf{Z}_{-[l]} = \mathbf{z}_{-[l]}, \sigma^2)}{(1 - \theta_l) f(\mathbf{y} | \mathbf{b}, Z_l = 0, \mathbf{Z}_{-[l]} = \mathbf{z}_{-[l]}, \sigma^2) + \theta_l f(\mathbf{y} | \mathbf{b}, Z_l = 1, \mathbf{Z}_{-[l]} = \mathbf{z}_{-[l]}, \sigma^2)} \\ &= \frac{\theta_l}{(1 - \theta_l) \frac{f(\mathbf{y} | \mathbf{b}, Z_l = 0, \mathbf{Z}_{-[l]} = \mathbf{z}_{-[l]}, \sigma^2)}{f(\mathbf{y} | \mathbf{b}, Z_l = 1, \mathbf{Z}_{-[l]} = \mathbf{z}_{-[l]}, \sigma^2)} + \theta_l}. \end{aligned}$$

Let  $\mathbf{B}_{ij} = (B_1(t_{ij}), B_2(t_{ij}), \dots, B_K(t_{ij}))'$  and  $g_{i,0}(t_{ij}) = \sum_{q \neq l} x_{qi} Z_q \mathbf{b}_{\cdot q}' \mathbf{B}_{ij}$  and  $g_{i,1}(t_{ij}) = x_{li} \mathbf{b}_{\cdot l}' \mathbf{B}_{ij} + \sum_{q \neq l} x_{qi} Z_q \mathbf{b}_{\cdot q}' \mathbf{B}_{ij}$ , so we have

$$\begin{aligned} & \frac{f(\mathbf{y} | \mathbf{b}, Z_l = 0, \mathbf{Z}_{-[l]} = \mathbf{z}_{-[l]}, \sigma^2)}{f(\mathbf{y} | \mathbf{b}, Z_l = 1, \mathbf{Z}_{-[l]} = \mathbf{z}_{-[l]}, \sigma^2)} \\ &= \exp \left\{ \frac{1}{2\sigma^2} \left[ \sum_{j=1}^{n_i} (y_{ij} - \beta_0(t_{ij}) - g_{i,1}(t_{ij}))^2 + \sum_{s \neq i} \sum_{j=1}^{n_s} (y_{sj} - \beta_0(t_{sj}) - g_i(t_{sj}))^2 \right. \right. \\ & \quad \left. \left. - \sum_{j=1}^{n_i} (y_{ij} - \beta_0(t_{ij}) - g_{i,0}(t_{ij}))^2 - \sum_{s \neq i} \sum_{j=1}^{n_s} (y_{sj} - \beta_0(t_{sj}) - g_i(t_{sj}))^2 \right] \right\} \\ &= \exp \left\{ \frac{1}{2\sigma^2} \left[ \sum_{j=1}^{n_i} (y_{ij} - \beta_0(t_{ij}) - g_{i,1}(t_{ij}))^2 - \sum_{j=1}^{n_i} (y_{ij} - \beta_0(t_{ij}) - g_{i,0}(t_{ij}))^2 \right] \right\} \\ &= \exp \left\{ \frac{1}{2\sigma^2} \left[ \sum_{j=1}^{n_i} (\tilde{y}_{ij} - g_{i,1}(t_{ij}))^2 - \sum_{j=1}^{n_i} (\tilde{y}_{ij} - g_{i,0}(t_{ij}))^2 \right] \right\}. \end{aligned}$$

Then,

$$\begin{aligned} P(Z_l = 1 | \mathbf{b}, \boldsymbol{\theta}, \boldsymbol{\mu}, \sigma^2, \boldsymbol{\tau}^2, \mathbf{Z}_{-[l]}, \mathbf{y}) &= P(Z_l = 1 | \mathbf{b}, \theta_l, \sigma^2, \mathbf{Z}_{-[l]}, \mathbf{y}) \\ &= \frac{\theta_l}{(1 - \theta_l) \exp \left\{ \frac{1}{2\sigma^2} \left[ \sum_{j=1}^{n_i} (\tilde{y}_{ij} - g_{i,1}(t_{ij}))^2 - \sum_{j=1}^{n_i} (\tilde{y}_{ij} - g_{i,0}(t_{ij}))^2 \right] \right\} + \theta_l}. \end{aligned} \quad (11)$$

The construction of the full conditional distribution of  $\sigma^2$  is already more straightforward. Taking into account that

$$\begin{aligned} f(\sigma^2 | \mathbf{b}, \boldsymbol{\theta}, \boldsymbol{\mu}, \boldsymbol{\tau}^2, \mathbf{Z}, \mathbf{y}) &\propto \pi(\sigma^2) \pi(\boldsymbol{\tau}^2) \pi(\boldsymbol{\mu}) f(\boldsymbol{\theta} | \boldsymbol{\mu}) f(\mathbf{b} | \sigma^2, \boldsymbol{\tau}^2) p(\mathbf{Z} | \boldsymbol{\theta}) f(\mathbf{y} | \mathbf{b}, \mathbf{Z}, \sigma^2) \\ &\propto \pi(\sigma^2) f(\mathbf{b} | \sigma^2, \boldsymbol{\tau}^2) f(\mathbf{y} | \mathbf{b}, \mathbf{Z}, \sigma^2) \propto \pi(\sigma^2) \left[ \prod_{k=1}^K \prod_{l=1}^p f(b_{kl} | \sigma^2, \tau_{kl}^2) \right] \left[ \prod_{i=1}^m \prod_{j=1}^{n_i} f(y_{ij} | \mathbf{b}, \mathbf{Z}, \sigma^2) \right] \\ &\propto \left( \frac{1}{\sigma^2} \right)^{\delta_1 + 1} \exp \left\{ -\frac{\delta_2}{\sigma^2} \right\} \left[ \prod_{k=1}^K \prod_{l=1}^p \left( \frac{1}{\sigma^2 \tau_{kl}^2} \right)^{\frac{1}{2}} \exp \left\{ -\frac{b_{kl}^2}{2\sigma^2 \tau_{kl}^2} \right\} \right] \\ &\quad \times \left[ \prod_{i=1}^m \prod_{j=1}^{n_i} \left( \frac{1}{\sigma^2} \right)^{\frac{1}{2}} \exp \left\{ -\frac{(y_{ij} - \beta_0(t_{ij}) - g_i(t_{ij}))^2}{2\sigma^2} \right\} \right] \\ \Rightarrow & \\ &f(\sigma^2 | \mathbf{b}, \boldsymbol{\theta}, \boldsymbol{\mu}, \boldsymbol{\tau}^2, \mathbf{Z}, \mathbf{y}) = f(\sigma^2 | \mathbf{b}, \boldsymbol{\tau}^2, \mathbf{Z}, \mathbf{y}) \\ &\propto \left( \frac{1}{\sigma^2} \right)^{\frac{\sum_{i=1}^m n_i}{2} + \frac{pK}{2} + \delta_1 + 1} \exp \left\{ -\frac{\sum_{i=1}^m \sum_{j=1}^{n_i} (\tilde{y}_{ij} - g_i(t_{ij}))^2 + \sum_{k=1}^K \sum_{l=1}^p \frac{b_{kl}^2}{\tau_{kl}^2} + 2\delta_2}{2\sigma^2} \right\}. \end{aligned} \quad (12)$$

Thus, the full conditional distribution of  $\sigma^2$  is an inverse gamma, with  $\frac{\sum_{i=1}^m n_i}{2} + \frac{pK}{2} + \delta_1$  as the shape parameter and  $\frac{\sum_{i=1}^m \sum_{j=1}^{n_i} (\tilde{y}_{ij} - g_i(t_{ij}))^2 + \sum_{k=1}^K \sum_{l=1}^p \frac{b_{kl}^2}{\tau_{kl}^2} + 2\delta_2}{2}$  as the rate parameter.

Finally, it remains to compute the full conditional for the  $\tau_{kl}^2$ 's. It is known that

$$\begin{aligned} f(\tau_{kl}^2 | \mathbf{b}, \boldsymbol{\theta}, \boldsymbol{\mu}, \sigma^2, \mathbf{Z}, \mathbf{y}) &\propto \pi(\sigma^2) \pi(\boldsymbol{\tau}^2) \pi(\boldsymbol{\mu}) f(\boldsymbol{\theta} | \boldsymbol{\mu}) f(\mathbf{b} | \sigma^2, \boldsymbol{\tau}^2) p(\mathbf{Z} | \boldsymbol{\theta}) f(\mathbf{y} | \mathbf{b}, \mathbf{Z}, \sigma^2) \\ &\propto \pi(\tau_{kl}^2) f(b_{kl} | \sigma^2, \tau_{kl}^2) \propto \frac{\lambda^2}{2} \exp \left\{ -\frac{\lambda^2}{2} \tau_{kl}^2 \right\} \left( \frac{1}{\sigma^2 \tau_{kl}^2} \right)^{\frac{1}{2}} \exp \left\{ -\frac{b_{kl}^2}{2\sigma^2 \tau_{kl}^2} \right\} \\ \Rightarrow & \\ &f(\tau_{kl}^2 | \mathbf{b}, \boldsymbol{\theta}, \boldsymbol{\mu}, \sigma^2, \mathbf{Z}, \mathbf{y}) = f(\tau_{kl}^2 | b_{kl}, \sigma^2) \\ &\propto \left( \frac{1}{\tau_{kl}^2} \right)^{\frac{1}{2}} \exp \left\{ -\left( \frac{b_{kl}^2}{2\sigma^2} + \frac{\lambda^2}{2} \tau_{kl}^2 \right) \right\}. \end{aligned} \quad (13)$$

With this structure, it is possible to prove that  $\eta_{kl}^2 = \frac{1}{\tau_{kl}^2}$ , when conditioned to the other terms of the hierarchical formulation it has normal-inverse distribution, with parameterization in  $\lambda'$  and  $\mu'$ , so that

$$f(x) = \sqrt{\frac{\lambda'}{2\pi}} x^{-\frac{3}{2}} \exp \left\{ -\frac{\lambda' (x - \mu')^2}{2(\mu')^2 x} \right\}, \quad x > 0.$$

To verify this, we need to rewrite the Expression (13) in terms of  $\eta_{kl}^2$ , including the Jacobian  $(-\frac{1}{(\eta_{kl}^2)^2})$ . So, the full conditional of  $\eta_{kl}^2$  is proportional to

$$\begin{aligned}
& (\eta_{kl}^2)^{-\frac{3}{2}} \exp \left\{ -\frac{1}{2} \left( \frac{b_{kl}^2}{\sigma^2} \eta_{kl}^2 + \frac{\lambda^2}{\eta_{kl}^2} \right) \right\} \\
& \propto (\eta_{kl}^2)^{-\frac{3}{2}} \exp \left\{ -b_{kl}^2 \left( \frac{\eta_{kl}^2}{2\sigma^2} + \frac{\lambda^2}{2\eta_{kl}^2 b_{kl}^2} \right) \right\} \\
& \propto (\eta_{kl}^2)^{-\frac{3}{2}} \exp \left\{ -\frac{b_{kl}^2 \left[ (\eta_{kl}^2)^2 + \frac{\lambda^2 \sigma^2}{b_{kl}^2} \right]}{2\sigma^2 \eta_{kl}^2} \right\} \\
& \propto (\eta_{kl}^2)^{-\frac{3}{2}} \exp \left\{ -\frac{b_{kl}^2 \left[ (\eta_{kl}^2)^2 - 2\eta_{kl}^2 \sqrt{\frac{\lambda^2 \sigma^2}{b_{kl}^2}} + \frac{\lambda^2 \sigma^2}{b_{kl}^2} \right]}{2\sigma^2 \eta_{kl}^2} \right\} \\
& \Rightarrow \\
& f(\eta_{kl}^2 | \mathbf{b}, \boldsymbol{\theta}, \boldsymbol{\mu}, \sigma^2, \mathbf{Z}, \mathbf{y}) = f(\eta_{kl}^2 | b_{kl}, \sigma^2) \\
& \propto (\eta_{kl}^2)^{-\frac{3}{2}} \exp \left\{ -\frac{b_{kl}^2 \left( \eta_{kl}^2 - \sqrt{\frac{\lambda^2 \sigma^2}{b_{kl}^2}} \right)^2}{2\sigma^2 \eta_{kl}^2} \right\}. \tag{14}
\end{aligned}$$

Then,  $\eta_{kl}^2$  has a normal-inverse distribution with  $\mu' = \sqrt{\frac{\lambda^2 \sigma^2}{b_{kl}^2}}$  and  $\lambda' = \lambda^2$ .

Thus, to simulate  $\tau_{kl}^2$  in the Gibbs sampler, it is enough to first simulate  $\eta_{kl}^2$  to then obtain  $\tau_{kl}^2$  through the transformation  $\tau_{kl}^2 = \frac{1}{\eta_{kl}^2}$ .

An additional account must be performed when considering  $\mu_l$  as a parameter:

$$\begin{aligned}
& f(\mu_l | \mathbf{b}, \boldsymbol{\theta}, \boldsymbol{\mu}_{-[l]}, \sigma^2, \boldsymbol{\tau}^2, \mathbf{Z}, \mathbf{y}) \\
& \propto \pi(\sigma^2) \pi(\boldsymbol{\tau}^2) \pi(\mu_l) \pi(\boldsymbol{\mu}_{-[l]}) f(\theta_l | \mu_l) f(\boldsymbol{\theta}_{-[l]} | \boldsymbol{\mu}_{-[l]}) f(\mathbf{b} | \sigma^2, \boldsymbol{\tau}^2) p(\mathbf{Z} | \boldsymbol{\theta}) f(\mathbf{y} | \mathbf{b}, \mathbf{Z}, \sigma^2) \\
& \Rightarrow \\
& f(\mu_l | \mathbf{b}, \boldsymbol{\theta}, \boldsymbol{\mu}_{-[l]}, \sigma^2, \boldsymbol{\tau}^2, \mathbf{Z}, \mathbf{y}) = f(\mu_l | \theta_l) \\
& \propto \pi(\mu_l) f(\theta_l | \mu_l) \propto I_{(0, \psi)}(\mu_l) \theta_l^{\mu_l} (1 - \theta_l)^{1 - \mu_l}. \tag{15}
\end{aligned}$$

Then,  $f(\mu_l | \mathbf{b}, \boldsymbol{\theta}, \boldsymbol{\mu}_{-[l]}, \sigma^2, \boldsymbol{\tau}^2, \mathbf{Z}, \mathbf{y})$  is a continuous bernoulli distribution with parameter  $\theta_l$  truncated on the interval  $(0, \psi)$ .